

Recent Achievements on the Physics of High- T_C Superconductor Josephson Junctions: Background, Perspectives and Inspiration

Francesco Tafuri · Davide Massarotti · Luca Galletti · Daniela Stornaiuolo · Domenico Montemurro · Luigi Longobardi · Procolo Lucignano · Giacomo Rotoli · Giovanni Piero Pepe · Arturo Tagliacozzo · Floriana Lombardi

Received: 10 September 2012 / Accepted: 21 September 2012 / Published online: 20 October 2012
© Springer Science+Business Media, LLC 2012

Abstract Coherent passage of Cooper pairs in a Josephson junction (JJ) above the liquid nitrogen temperature has been the first impressive revolutionary effect induced by high critical temperature superconductors (HTS) in the domain of the study of Josephson effect (JE). But this has been only the start. A d -wave order parameter has led to significant novel insights in the physics of the JE turning into a device the notion of a π -junction. Spontaneous currents in a frustrated geometry, Andreev bound states, long-range proximity effect have rapidly become standard terms in the study of the JE, standing as a reference bench for conventional systems based on low critical temperature superconductors (LTS) and inspiring analogies for junctions based on novel

superconductors discovered in the meantime. The extreme richness of the physics of HTS JJs has not been adequately supported by the expected impact in the applications, the main reason lying in the complexity of these materials and in the consequent unsatisfactory yield and reproducibility of the performances of the JJs within the required limits. The continuous progress in material science, and specifically in the realization of oxide multi-layers, and in nanotechnologies applied to superconductors, accompanied by the advances in a better understanding of the properties of HTS and of HTS devices, has as a matter of fact opened possible novel scenarios and interest in the field. We intend to give a brief overview on interesting new problems concerning HTS JJs of inspiration also for other systems. We also review some ideas and experimental techniques on macroscopic quantum decay phenomena occurring in Josephson structures. The attention is mainly addressed to intermediate levels of dissipation, which characterize a large majority of low critical current Josephson devices and are therefore an unavoidable consequence of nanotechnology applied more and more to Josephson devices.

F. Tafuri (✉) · L. Longobardi · G. Rotoli
Dip. di Ingegneria dell'Informazione, Seconda Università degli Studi di Napoli, via Roma 29, 81031 Aversa (Ce), Italy
e-mail: tafuri@na.infn.it

F. Tafuri · D. Massarotti · L. Galletti · D. Stornaiuolo · G.P. Pepe · A. Tagliacozzo
CNR-SPIN, Complesso Universitario di Monte S. Angelo, 80126 Napoli, Italy

D. Massarotti · L. Galletti · D. Stornaiuolo · P. Lucignano · G.P. Pepe · A. Tagliacozzo
Dip. Scienze Fisiche, Università di Napoli Federico II, Complesso Universitario di Monte S. Angelo, 80126 Napoli, Italy

D. Montemurro
NEST-Scuola Normale Superiore and Istituto Nanoscienze-CNR, Piazza San Silvestro 12, 56127 Pisa, Italy

P. Lucignano
CNR-ISC, via Fosso del Cavaliere 100, 00133 Roma, Italy

F. Lombardi
Dept. of Microtechnology and Nanoscience, Chalmers University of Technology, 41296 Göteborg, Sweden

Keywords Josephson effect · High T_C superconductors · Macroscopic quantum phenomena · Nanostructures

1 Introduction

An overview on manuscripts focused on superconductivity reveals a large variety of themes and an amazing amount of different superconducting materials. Probably, superconductivity has never been so rich with materials and problems! On conventional low critical temperature superconductors (LTS) there is a continuous work of optimizing the

quality of samples and of junctions, of interfaces and nanostructures, while ‘exotic’ superconductivity counts not only high critical temperature superconductors (HTS) [1]. Heavy fermions, organic superconductors, fulleride superconductors, rutheno-cuprates, magnesium diborides, iron-based superconductors are examples of classes of materials with ‘unconventional’ superconductivity. We will not enter into the details of their phenomenology and of their physics, for which excellent work and reviews are obviously available in literature. We simply intend to review some recent advances in the realization and the study of Josephson junctions (JJs) and nano weak links based on HTS, aware that the know-how acquired on HTS may be inspiring to produce Josephson devices for any of these materials.

If we go back in time and imagine to be a few months before the discovery of HTS, who would have imagined that in a few weeks a supercurrent would have flown up to about 100 K? And who would have imagined in a Josephson junction a supercurrent between two phase coherent electrodes up to about 100 K? How do fluctuations work at these high temperatures? How conceivable is to accept coherence lengths not larger than a couple of nanometers? These considerations lead to the first obvious feature on HTS, which is independent of their still debated origin of superconductivity and of their very complicate structure: HTS oxides enlarge the occurrence of superconductivity to unexpected energy and length scales. This is obviously true also for the Josephson effect. Dimensionality, strong correlations, *d*-wave order parameter (OP) symmetry will represent the other ingredients which contribute to define the properties of HTS. HTS have really opened the new horizons of unconventional superconductivity, where probably all bundles will converge for a more complete understanding of its nature.

The Josephson effect (JE) [2–6] has been in the last 50 years a continuous source of inspiration and progress in physics. We have been learning through the JE how macroscopic coherence propagates in hetero-structures [3–9], how macroscopic and microscopic phases coherently combine at superconductor/normal metal (S/N) interfaces [10–14] of a S/N/S JJ, how a Josephson coupling can unambiguously identify unconventional symmetry of the order parameter, as occurring in HTS [15, 16]. The intrinsic and robust quantum nature of the JJs is also the basis of well-established applications such as the superconducting quantum interference devices (SQUIDs) [4, 17] and of a prospective hybrid architecture for quantum information [18]. These are just a few examples chosen from a multitude of possibilities.

We will consider aspects on the physics of the JE in HTS focussing on more recent developments, ranging from escape dynamics and macroscopic quantum tunneling to mesoscopic effects, as well as the realization and the physics of nano-structures and hybrid devices, the new frontiers opened by nanotechnology. We look at escape dynamics

aware that material science is not only offering a variety of novel interfaces and junctions, but also radically new solutions of synthesizing hybrid Josephson devices, taking advantage at the same time of the progress registered in using nanotechnologies in superconducting electronics. Escape dynamics at intermediate levels of dissipation (moderately damped regime) is going to permeate more and more the nature of futuristic superconducting hybrid nanostructures. The first part of this contribution will be devoted to revisit some of the concepts that have appeared as unique signatures of unconventional superconductivity and in our opinion of inspiration for the physics of devices based on novel classes of exotic superconductors. Terms as for instance π -phase shift junction, Josephson coupling across grain boundaries (GBs), Andreev bound states, fractional vortices, time-reversal symmetry breaking in the JE have become more popular terms since the advent of HTS JJs. Several excellent reviews of various aspects of weak links have appeared previously. This contribution is more our point of view rather than an exhaustive review. We hope to build upon previous work and apologize in advance for work that we neglect.

2 Different Types of HTS Josephson Junction

Because of the difficulties in producing a traditional trilayer structure (superconductor–insulator (normal metal)–superconductor, S–I (N)–S) composed by HTS electrodes [19, 20], in analogy to LTS JJs alternative types of junction have been developed. The HTS junctions are described in extensive reviews [19–21] with all proper references. Here we briefly outline the main concepts of those junctions employed in the experiments described in the following.

2.1 Grain Boundary Junctions

Grain boundary (GB) junctions have been largely used in HTS compounds. They take advantage of a significant reduction of the critical current between two grains with different orientations which generates weak coupling and Josephson-like behavior between the two electrodes. The bicrystal technique, based on the union of two substrates with different crystal orientations, is the most direct way to create a GB [22–24]. The HTS films, if they grow epitaxially, will reproduce the relative orientations of each of the two substrates. Originally applied to $\text{YBa}_2\text{Cu}_3\text{O}_{7-x}$ (YBCO) GB technique has been extended to a large number of HTS materials and has been the first approach to junctions of other materials, as for instance iron pnictides [25–27], or reference for systems [28] where it is much easier to grow a barrier as in magnesium diboride [29–33].

Bicrystal imposes junctions on specific locations determined by how the substrates are glued. Methods to locate

GB junctions everywhere on a chip were offered for HTS by the step, step-edge and biepitaxial techniques, all employing photolithographic means to define the GB interfaces (plenty of references can be found in review papers [19, 20]). The biepitaxial technique for instance uses changes of the orientation of HTS films induced by epitaxial growth on structured template layers. In the original technique [34], a MgO template layer on a *r*-plane sapphire produces an in-plane rotation by 45° of a SrTiO₃/YBCO bilayer compared to an identical bilayer grown directly on the sapphire, producing a GB with a 45° tilt around the [001] direction. The biepitaxial technique has been extended to novel configurations, in which one of the electrodes does not grow along the *c*-axis orientation [35–39]. A (110)-oriented MgO or CeO₂ buffer layer is deposited on (110) SrTiO₃ [35–39] or (La_{0.3}Sr_{0.7})(Al_{0.65}Ta_{0.35})O₃ (LSAT) substrates [40]. YBCO grows along the [001] direction on the MgO and on the CeO₂ seed layers, while it grows along the [103]/[013] direction on SrTiO₃ or LSAT substrates. The presence of the CeO₂ produces an additional 45° in-plane rotation of the YBCO axes with respect to the in-plane directions of the substrate. As a consequence, the GBs are the product of two 45° rotations, a first one around the *c*-axis, and a second one around the *b*-axis. Atomically flat interfaces can be achieved in appropriate conditions [35–37], as a result of an opportune “self-assembling” growth mode. The tilt of one of the electrodes and the in-plane 45° rotation on the CeO₂ both contribute to decrease the barrier transmission, while the in-plane rotation enhances on demand the desired *d*-wave features (see next section). These types of junction have been used for the macroscopic quantum tunneling experiments [41–43] discussed below.

Recent improvements in the quality of step-edge junctions, also through a systematic study of morphological properties, provide $I_C R_N$ values comparable to the best results reported for [100]-tilt HTS [44, 45]. The fact that $I_C R_N$ quality factors remain definitely lower than the expected gap of HTS compounds has been one of the major problems since the beginning (see references in [19, 20]). There are no radically new results in the last few years on how to improve $I_C R_N$, but more controlled junctions seem to favor an increase of $I_C R_N$ as also confirmed by studies on submicron biepitaxial JJs reported in Sect. 6 [40, 46].

GBs have been used for several corner-stone experiments on HTS junctions [15, 19, 20]. The possibility to span over four orders of magnitude in the critical current density (J_C) and the normal state resistance (R_N) by selecting specific misorientation angles in GB junctions remains as one of the most significant advantages. This is mostly ruled by the *d*-wave OP symmetry and by the GB microstructure. We can have on one hand large J_C values for relatively low misorientation angles, which allow studies on static and dynamical effects associated to half-flux quantization. On the other

hand J_C values of the order of 10² A/cm² lead to junctions with hysteretic behavior in the current-voltage characteristics, which have permitted the macroscopic quantum experiments discussed later.

2.2 Junctions with an Artificial Barrier

The complexity of HTS compounds and the difficulty of creating good quality interfaces stand as major problems for the possible development of a reliable and desirable tri-layer technology, independently of the type of barrier, i.e. noble metals or oxide-like materials. Junctions employing a LTS counter-electrode definitely have better performances than those employing HTS thin films for both electrodes, but are obviously limited in their working temperature range. We will recall a few examples of functional devices of this type developed up to now (referring to [20] for an extensive list and discussion). We believe that advances gained in realizing and characterizing oxide heterostructures [47–50] might be inspiring to revisit also some concepts for the fabrication of oxide junctions. They might offer alternatives to the main routes followed up to now, mostly aimed to reduce lattice mismatches [51].

While GB junctions are only based on thin films, junctions with artificial barriers have been made on both thin films and single crystals. The first YBCO (single crystal)-insulator-Pb (Nb) junctions [52–54] have been promptly replaced by a second generation based on thin films [55, 56]. Barriers have been fabricated using different methods. The most frequent solution uses a junction fabrication process with “ex-situ” steps, consisting of an external chemical or ion milling etching. An example is provided by ramp-type junctions, which use the well-established *c*-axis HTS thin-film technology while allowing the main current to flow in the *a*–*b* planes [56]. Noble metal barriers also serve to prevent oxygen diffusion and to lower the junction resistance. In the YBCO-Nb junctions [56], for instance, a 7-nm YBCO interlayer and an Au layer typically ranging between 6 and 12 nm were used as a barrier. By adjusting the Au-barrier thickness *d*, the critical current density J_C can be tuned over a wide range from 10 A/cm² ($d = 120$ nm) up to values of 10⁵ A/cm² ($d = 7$ nm).

In “in-situ” junctions three layers are deposited without any exposure to atmosphere [57–59]. The most significant step in the direction of the goal of an all-HTS tri-layer with an insulating barrier is the structure composed of La_{1.85}Sr_{0.15}CuO₄ (LSCO) electrodes separated by a one-unit-cell-thick La₂CuO₄ (LCO) barrier [57]. In the LSCO junctions, the LCO barrier thickness ranged from 1 to 15 unit cells (up to 20 nm). Inhomogeneous currents flow at low temperatures [60]. This experiment converted the junction from S–N–S to S–I–S through annealing at low temperature in vacuum, which drives LCO insulating leaving LSCO

almost intact [60]. Concerns about the coexistence of superconductivity and anti-ferromagnetism, verifiable through measurements on the JE [61, 62], have been raised by these experiments [57].

Long-range or anomalous proximity effect has also been discussed for other types of junction (see for instance references in Ref. [60]), and within the context of quantum phase transitions between the low carrier-concentration insulating antiferromagnetic phase and the high carrier-concentration metallic and superconducting phase [63]. The ability of a giant barrier to transfer a Josephson current has been attributed to the inhomogeneous nature of the barrier and the presence of superconducting islands embedded in the normal metallic matrix [64]. This is a potential argument of general interest.

2.3 Intrinsic Josephson Junctions

The layered crystal structure with strongly anisotropic properties in HTS allows another “unique” type of junction called intrinsic stacked junctions. These junctions mostly exploit *c*-axis transport. Most successful results have been achieved in Bi₂Sr₂CaCu₂O₈ [65] and Tl₂Ba₂Ca₂Cu₃O₁₀ single crystals and thin films [66, 67]. Josephson coupling between CuO₂ double layers has been proved, and most of the materials behaved like stacks of S-I-S JJs with effective barriers of the order of the separation of the CuO₂ double layers (1.5 nm) (J_C typically 10³ A/cm²) [68]. Practical realizations of IJJ have been designed in order to nominally avoid heating effects [68–70].

3 The Josephson Effect and the Order Parameter Symmetry

Probably the most convincing evidence for a predominantly $d_{x^2-y^2}$ pairing symmetry in the cuprates has come from phase sensitive tunneling measurements [15, 16, 53, 54, 71]. Evidence from other types of measurement have been extensively discussed in [15]. After the first two spectacular phase sensitive tunneling demonstrations of the *d*-wave nature of the OP symmetry in HTS [53, 54, 71], other experiments still employing JJs have confirmed the effectiveness of a predominant *d*-wave OP symmetry. The whole set of experiments now constitutes a solid background [15, 16, 19, 20] whose methodology and procedures can be extended to junctions composed of whatever type of materials. This does not apply only to unconventional materials, where it would make sense to look for ‘exotic’ OP symmetry but also for instance to junctions with ferromagnetic barriers, whose unconventional phenomenology also funds on the notion of π -phase shift [72–77].

3.1 Current–Phase Relation and the Notion of π Phase Shift

The general expression of the current–phase relation which takes into account current components carried by multiple reflection processes at the junction interface and effects related to possible anisotropic OP symmetry, is [13, 71, 78]

$$I(\phi, \theta_1, \theta_2) = \sum_{n \geq 1} (I_n(\theta_1, \theta_2) \sin(n\phi) + J_n(\theta_1, \theta_2) \cos(n\phi)) \quad (1)$$

where θ_1 and θ_2 are the angles of the crystallographic axes with respect to the junction interface of the left and right electrodes, respectively. The I_n contribution depends on the barrier transparency as a \bar{T}^n power-law and corresponds to the *n*-multiple reflection process. On the basis of general symmetry arguments, for two generalized *d*-wave superconductors in the case of time-reversal symmetry $J_n = 0$, to the lowest order, the well known Sigrist–Rice expression is found in the clean limit [79]:

$$I(\phi, \theta_1, \theta_2) = A_S [\cos(2\theta_1) \cos(2\theta_2)] \cdot \sin(\phi). \quad (2)$$

The dirty limit expression when disorder effects and faceting are taken into account, is

$$I(\phi, \theta_1, \theta_2) = A_S [\cos(2\theta_1 + 2\theta_2)] \cdot \sin(\phi). \quad (3)$$

In these expressions a negative supercurrent can be translated as a phase shift of π at the junction [80].

Particular choices of θ_1 and θ_2 (for instance with a misorientation of 45° in GB junctions) can also make the $\sin(\phi)$ component negligible. Higher order corrections in the current-phase relation can lead to important modifications for *d*-wave superconductors.

The free energy can be expressed as

$$F_J = -\Phi_o / (2\pi c) |I_1| \cos(\phi - \phi_o), \quad (4)$$

which is not invariant under time reversal. The intrinsic phase shift is ϕ_o , which corresponds to a two-fold degenerate state which breaks time-reversal symmetry. A direct consequence of time-reversal symmetry breaking can be seen in the presence of spontaneous supercurrents and the possibility of vortices with fractional flux quanta [81, 82]. Again these concepts extensively studied for HTS [15, 20, 81] are of general relevance for all exotic superconductors, and recently also for systems aimed to the detection of Majorana fermions [83–94], with some intriguing merging of the physics of Majorana bound states and of *d*-wave JJs, with their additional intrinsic possibility of manipulating the phase [92].

Deviations from the sinusoidal behavior are relevant for weak links in the ballistic case at low temperatures and for highly transmissive barriers [5, 6, 96, 97]. Issues related to I_C – ϕ for different types of junction have been extensively discussed in the review by Golubov, Kupryanov and

Ilichev [95]. I_C - ϕ measurements on high angle bicrystal GB junctions, especially in 45° asymmetric and 45° symmetric configurations, have reported the prevalence of the 2ϕ component under some specific conditions [98–101]. In RF measurements the sample is inductively coupled to a high-quality parallel resonance circuit driven at its resonant frequency. The observation of integer as well as subharmonic constant voltage steps at $V_{n,m} = \frac{n}{m} \frac{h}{e} v$, with n and m integer numbers (fractional Shapiro steps) [102, 103] have not been considered up to now an unambiguous proof of the presence of the second harmonic since measured effects can also result from a GB being composed of multiple junctions in parallel [103]. The possibility of concomitant processes manifesting in fractional Shapiro steps should be also taken into account in recent proposals aimed to detect Majorana fermions [83–88].

3.2 Evidence for d -Wave Symmetry from Tunneling Measurements

We refer the readers to original fonts and extensive reviews for a detailed discussion and historical account [15, 16], here we are interested to briefly recall the main concepts.

3.2.1 The Origins and the First Phase Sensitive Tests

The basis for phase sensitive tests of the pairing symmetry in superconductors was suggested by Bulaevskii et al. in 1977 [104]. They proposed that it is possible to have an intrinsic phase shift of π in a superconducting loop including a Josephson junction, in the absence of an externally applied field or current (π -ring), the origin of the effect being spin-flip assisted tunneling within the tunnel junction itself. The first proposal to introduce a π -phase shift into a superconducting ring by taking advantage of the momentum dependence of the pairing wave function in unconventional superconductors has been demonstrated by Geshkenbein, Larkin and Barone [105, 106]. They suggested using the properties of π -rings to test for unconventional pairing symmetry in the heavy fermion superconductors [105, 106]. Sigrist and Rice [79] proposed that the paramagnetic Meissner effect [15, 107] which occurred in ceramic samples of $\text{Bi}_2\text{Sr}_2\text{CaCu}_2\text{O}_8$ was due to naturally occurring π -rings due to Josephson contacts between the grains, and suggested using a controlled geometry as a test of d -wave superconductivity in the HTS. A π -phase shift can be also induced by other mechanisms, by tunneling through ferromagnetic layers [72, 73, 108], and by running supercurrent through two closely spaced electrodes along the ring [109, 110].

The controlled geometries that have been used for observing the effects of an intrinsic π -shift in a superconducting ring can be divided into two classes. In the first, the 0 - π junction, one section of a JJ has an intrinsic π phase shift

relative to the other. A second geometry for phase sensitive tests of the pairing symmetry in unconventional superconductors is the SQUID, a superconducting ring with at least one JJ, with in general an intrinsic phase shift ϵ upon circling the ring [15, 16]. The first such experiments were by Wollman et al. [53, 54]. They made π -rings and 0 - π junctions between single crystals of YBCO and Pb, a conventional superconductor. They observed a phase shift of π in the dependence of the critical currents of their π -SQUIDS on applied flux, relative to that expected for a conventional SQUID, and they observed a minimum in the critical current of their 0 - π junctions at zero applied field. Later experiments achieved better quantitative agreement due to improvements in the control on the asymmetries in the junction critical currents or inhomogeneities in the junction I_C densities [111].

The first experiments to detect the spontaneous flux predicted for π -SQUIDS and 0 - π junctions fabricated from cuprate superconductors were by Tsuei et al. [15, 71]. They formed π -rings and 0 - π junctions using a tricrystal geometry with GB weak links [15, 71] and observed a neat spontaneous magnetizations of about $\Phi_0/2$. These spontaneous currents were imaged with a scanning SQUID microscope [15]. More recently, large arrays of π -rings [56] were realized by using ramp-edge junction technology of YBCO-Nb described above and taking advantage of the large currents. Spontaneous generation of half-flux quantum vortices in 0 - π junctions was observed at each facet corner as the sample through scanning SQUID microscopy [112, 113]. The directions of circulation of the spontaneous supercurrents order strongly antiferromagnetically when the facet corners are electrically connected, but only weakly when the facet corners are electrically disconnected.

In recent years the use of scanning magnetic microscopies ranging from SSM (just discussed for HTS cuprates) to scanning Hall bar microscopy (SHM) and magnetic force microscopy (MFM) have been largely applied to a variety of problems including the physics of novel superconductors [114]. Studies both aimed to static imaging mode and to vortex dynamics have been realized. Apart from studies on the search of spontaneous magnetization also in ruthenocuprates [115–117], where triplet pairing with broken time-reversal symmetry is expected [118, 119], and possible interest for eutectic samples $\text{Sr}_2\text{RuO}_4/\text{Sr}_3\text{Ru}_2\text{O}_7$ [120], examples are: the static imaging of magnetic flux in wire lattices, clusters and arrays of rings and nanoholes, the observation of Pearl vortices [121], unusual flux arrangements observed in magnetic superconductors, fluxoid dynamics for the spin-charge separation problem [114], the direct imaging of the coexistence of ferromagnetism and superconductivity at the $\text{LaAlO}_3/\text{SrTiO}_3$ interface [122], the measurement of superconducting fluctuations on samples comparable in size to the coherence length, revealing for instance stripes in the pnictide superconductor Co doped Ba-122 and the presence of

spin-like excitations [123]. All this is discussed in detail in the review by Kirtley [114], which also deals with issues associated to HTS.

3.2.2 Pairing Symmetry in the Behavior of Single Josephson Junctions

Pairing symmetry of the cuprate superconductors from the dependence of the I_c of HTS JJs on junction angle relative to the cuprate crystalline axes was also inferred by using two very different junction technologies. Lombardi et al. [38] have measured the angular dependence of the Josephson I_c of c -axis tilt biepitaxial GB YBCO junctions based on a CeO₂ seed layer, while Smilde et al., [124] have used the YBCO-Nb ramp-edge technology to produce a series of junctions with varying junction normals relative to the a -axis. The former experiment is realized in an all HTS system and uses junctions with much lower J_C . “Intrinsic” d -wave effects are dominant in the phenomenology of the JJs themselves (not inserted in any loop) independent of the interface details. On the same type of GB junctions scaled to the submicron size [46], a closer correspondence with the ideal Sigrist–Rice formula is found for the dependence of the I_c on the interface angle. This signifies that submicron scaling gives access to a more “intrinsic” nature of GB junctions, rendering more homogeneous the narrower barrier composed of only few facets, where the scattering is expected to be more uniform [46]. The low barrier transmission probabilities, which preserves the directionality of the Cooper pairs, are probably the inner reason for the robustness of the observed effects, preserved on a scale larger than the faceting and/or any interface impurity characteristic lengths.

In the latter experiment the junctions were made with either twinned or untwinned YBCO films [125], and deviations expected for untwinned YBCO samples were consistently observed. The presence of a small imaginary component to the gap [15, 112, 113, 124] has been largely debated since early times, with several insights coming also from tunneling spectroscopy [15, 21]. No consensus exists up to now. The component if any, is, however, small. Novel insights can arise through spectroscopic measurements [126] on meso/nano islands. Concepts and methodologies used for HTS junctions and discussed above can be obviously applied to weak links of any materials.

Predominantly d -wave pairing symmetry has been also inferred from the characteristics of asymmetric 0–45° c -axis twist junctions, which have rapidly alternating 0- and π -junctions due to faceting. Such faceting results in unusual magnetic interference patterns [19, 20, 127–129] and spontaneous flux generation in the grain boundaries [128–131]. The rapid alternation in sign of the local Josephson critical current due to faceting can result in “splinter” Josephson

fluxons with flux a fraction of the conventional flux quantum [132, 133]. Splinter vortices form pairs with magnetic fluxes that sum to Φ_0 and originate on a background of a dense linear array of interchanging 0 and π junctions, where magnetic flux associated with spontaneous currents with random orientation is basically unquantized. These magnetic structures can be classified as fractional vortices. While fractional vortices might be correlated with time-reversal symmetry breaking (BTRS), and possibly with the presence of an imaginary component of the OP, the existence of splinter vortices does not depend on the presence of any imaginary component of the order parameter [132, 133].

The fact that Andreev bound states (ABS) and/or proximity effect could produce BTRS without an imaginary component of the OP [134–138] motivated attempts to see spontaneous flux and fractional vortices in systems without GBs [139, 140]. If translation symmetry is broken, the superconducting state spontaneously generates a current and a magnetic field. For instance, spontaneous currents have been observed to be spatially correlated with impurities due to the presence of the so-called green phase, due to Y excess in c -axis films [140]. However, the origin of such currents is unclear. It may be due to BTRS, to an imaginary component of the order parameter or to the spontaneous nucleation of topological defects in phase transitions, for instance the pinning of a vortex tangle, produced near T_c in a Berezinskii–Kosterlitz–Thouless [141, 142] type transition in the nearly two-dimensional superconductor YBCO.

Another way of investigating BTRS at interfaces is through tunneling spectroscopy, and more specifically the study of zero-energy bound states, which are detected through a peak at zero voltage (zero bias conductance peak ZBCP) [13, 21, 144–146]. Point-contact and scanning tunneling microscopy (STM) measurements, which provide measures of the quasiparticle density of states, give further evidence for unconventional pairing symmetry in the cuprate superconductors. It is beyond the scope of this review to cover this vast topic in detail, that would also lead the very interesting case of electron-doped HTS [15] and parent-structure HTS [147]. We refer the reader to extensive reviews [21, 143].

In conclusion, the enormous amount of work made to evaluate if all junction properties would be consistent with a d -wave OP symmetry represents a very strong and solid background, and provides clear methodologies to test the nature of the OP symmetry in whatever type of junctions. From the analysis of the magnetic pattern, for instance, we are now able to simulate more and more anomalous behavior with respect to the LTS standards [4] by taking into account particular morphologies of the electrodes, unconventional symmetry of the OP, the two-dimensional nature of the electrodes, even in the case one-dimensional barriers, and so on. In other words HTS have somehow changed the

terms and the perception of what is really unconventional when referring to the properties of a Josephson junction and contributed to establish some criteria for ‘novel’ standards.

4 Escape Dynamics: the Origins and Macroscopic Quantum Tunneling

Once outlined how classical responses of the Josephson phenomenology were modified in HTS junctions as a consequence of the specific microstructure or of an unconventional OP symmetry, probably one of the most significant advances has been the recent reconstruction of the phase dynamics of HTS JJs. This has been performed through a series of experiments aiming at measuring quantum escape and demonstrating macroscopic quantum tunneling (MQT). Even in absence of a clear picture of the transport modes and of how proximity effect microscopically works at HTS junction’s interface, the possibility of describing escape dynamics, sensitive fingerprint of the physics of the JJ, in terms of the parameters commonly used in LTS devices is a relevant step. The occurrence of MQT in *d*-wave junctions is of particular significance for the study of the macroscopic quantum phenomena, where low-energy quasiparticles are expected to induce dissipation and spoil macroscopic coherence.

The study of escape dynamics in JJs got most of its experimental fundamentals in the 1980s and has always represented one of the most relevant and fascinating topics, which in the last decade turned out to be essential in the realization of qubits [18].

Considerable insights into the non-linear dynamics of a JJ can be gained by realizing that the equation resulting from the Resistively Shunted Junctions (RSJ) model [3–6]

$$\left(\frac{\Phi_o}{2\pi}\right)^2 C \frac{\partial^2 \phi}{\partial t^2} + \left(\frac{\Phi_o}{2\pi}\right)^2 \frac{1}{R} \frac{\partial \phi}{\partial t} + \frac{\partial}{\partial \phi} U = 0 \tag{5}$$

where

$$U = -\Phi_o/(2\pi)(I_C \cos(\phi) + I\phi) \tag{6}$$

with Φ_o the flux quantum and I_C the critical current, describes the motion of a ball moving on the ‘tilted washboard’ potential U (see Fig. 1a). The term involving the capacitance C represents the mass of the particle, the $1/R$ term represents the damping of the motion, and the average ‘tilt’ of the washboard is proportional to $-I$. The strength of the friction can be also expressed through the junction quality factor $Q = \omega_p RC$, where $\omega_p = (2eI_C/\hbar C)^{1/2}(1 - \iota^2)^{1/4}$ is the plasma frequency being $\iota = I/I_C$.

When the bias current is ramped from $\iota = 0$ to $\iota < 1$, the junction is in the zero-voltage state in absence of thermal and quantum fluctuations and the particle is confined to one of the potential wells, where it oscillates back and forth at

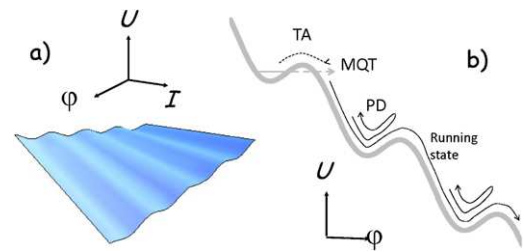


Fig. 1 (a) Three-dimensional view of washboard potential in the RSJ model as a function of the phase and of the bias current. The current spans from 0 to I_C . (b) A two-dimensional cut from (a) for a fixed value of the current. TA stands for thermal activation (black dotted line), while MQT for macroscopic quantum tunneling (grey dotted line). Once the particle/phase overcomes the barrier, it rolls in the running state. Retrapping processes may happen for intermediate levels of dissipation determining a phase diffusion (PD) regime

the frequency ω_p . At finite temperature, the junction may switch into a finite voltage state for a bias current $\iota < 1$. This corresponds to the particle escaping from the well either by a thermally activated (TA) process [148] or by tunneling through the barrier potential, known as MQT [7–9, 18] (see Fig. 1b). The MQT rate is thus affected by dissipation, because of the damping dependent factor [7–9, 149]. Once the phase point gets over a hill by fluctuations, it keeps running, provided that the damping is below some critical value.

The very first experiments on MQT in a JJ were carried out by Voss and Webb [150] and by Jackel et al. [151], while related experiments on a junction inserted in a superconducting loop were realized by de Bruyn Ouboter et al. [152, 153], Prance et al. [154] and Dmitrenko et al. [155]. The temperature dependence of the effect of damping on the tunneling has been addressed by later experiments [156, 157]. Devoret, Martinis and Clarke [158–160] have established a detailed conceptual and experimental protocol to follow to prove the macroscopic quantum nature of tunneling and its crossover to the thermal regime, used in most of later experiments. It has been clearly addressed the problem of the complex impedance presented to the junction at microwave frequencies by the wires directly connected to it or by any circuit in its vicinity, and classical phenomena have been used to measure all relevant parameters of the junction in situ [158–160]. I_C and shunting admittance were determined in situ in the thermal regime from the dependence of escape rate Γ on bias current and from resonant activation in the presence of microwaves. In a further series of experiments, the existence of quantized energy levels in the potential well of the junction was demonstrated spectroscopically [158–160]. The behavior of the phase difference ϕ is deduced from measurements of Γ of the junctions from its zero-voltage state. To determine the escape rate 10^4 – 10^5 events are typically collected for each set of parameters. The resulting distribution of the switching probability $P(I)$ is

used to compute the escape rate out of the zero-voltage state as a function of the bias current I [161].

In the pure thermal regime, the escape rate for weak to moderate damping ($Q > 1$) is determined by [148]

$$\Gamma_t(\iota) = a_t \frac{\omega_p}{2\pi} \exp\left(-\frac{\Delta U(\iota)}{k_B T}\right), \quad (7)$$

where $\Delta U(\iota) = (E_J 4\sqrt{2}/3)(1 - \iota)^{3/2}$ is the barrier height for ι close to one and $E_J = \hbar I_C / 2e$ is the Josephson energy. The escape rate will be dominated by MQT at low enough temperature [7–9, 149]: for $Q > 1$ and ι close to one it is approximated by the expression for a cubic potential,

$$\Gamma_q(\iota) = a_q \frac{\omega_p}{2\pi} \exp\left[-7.2 \frac{\Delta U(\iota)}{\hbar\omega_p} \left(1 + \frac{0.87}{Q}\right)\right], \quad (8)$$

where $a_q = (864\pi \Delta U / \hbar\omega_p)^{1/2}$.

It is convenient to express the thermal and the quantum escape through an escape temperature T_{esc} defined as

$$\Gamma_{t,q}(\iota) = \frac{\omega_p}{2\pi} \exp\left[-\frac{\Delta U(\iota)}{k_B T_{\text{esc}}}\right]. \quad (9)$$

The crossover temperature T_{cr} between the thermal and quantum regimes is given by $T_{\text{cr}} = (\hbar\omega_p / 2\pi k_B) \{(1 + 1/4Q^2)^{1/2} - 1/2Q\}$.

The shunting capacitance dominate the self-capacitance of the junction, while the bias circuitry determine the shunting conductance, respectively. The magnetic field has been used as a crucial knob to tune T_{cr} by changing the critical current and therefore the plasma frequency.

Following an event of escape the particle may travel down the potential for a few wells and then be retrapped in one of the following minima of the potential [162, 163]. At low bias the process of escape and retrapping may occur multiple times generating extensive diffusion of the phase until an increase of the tilt of the potential, due to a change in the bias current, raises the velocity of the particle and the junction can switch to the running state [43, 69, 70, 162–168]. The transition from thermal activation (TA) (with the expected dependence of width σ of the switching current distribution on the temperature, $\sigma \propto T^{2/3}$) to underdamped phase diffusion (PD) regime is marked by the collapse of σ and the turn over temperature T^* is defined as the temperature at which the width σ of the switching current distribution (SCD) reaches the maximum value. When increasing the temperature, histograms tend to become more symmetric and shrink rather than broaden with a consequent increase of their maximum amplitude. This translates into a characteristic dependence of σ , i.e. appearance of an anticorrelation between the temperature and the width of the switching distributions [69, 70, 164–168]. The change in the sign of the derivative of the second moment of the distribution and a modification of the shape of the distributions at temperatures around T^* turn to be distinctive signatures of the PD regime.

When the junction is not in the MQT regime, a temperature increase enhances the possibility of a switching at lower currents. The dependence of the mean value of the SCD (i.e. the mean switching current I_{SW}) on the temperature is a fingerprint of the dynamics of the junction and changes in the transition from TA regime to PD. Due to the onset of re-trapping events, it is necessary to provide a larger tilt to the energy potential to allow the system to switch to the running state. Therefore, above T^* the experimental values of I_{SW} are greater than the predicted values, which only consider the effects of TA.

In Fig. 2a,b SCD histograms are schematized in the low and moderate damping regime, respectively. They give an intuitive representation of the quite different features, along with the temperature dependence of σ and I_{SW} as discussed above.

5 Escape Dynamics in ‘Novel’ Types of Junction, the Case of High- T_C Compounds

Studies on macroscopic quantum behavior have been in the last few years extended to novel types of structure and material. We will refer as novel types of junction, those composed of novel materials, or devices scaled to the nano-size or based on novel design concepts, as intrinsic junctions in HTS or junctions using nanowires as barriers. SCD measurements have turned to be standard tools to investigate phase dynamics in unconventional and hybrid systems and nano-structures. HTS are an example of unconventional systems, because of the d -wave OP symmetry and of the presence of low-energy quasiparticles [15]. Low-energy quasiparticles have represented since the very beginning a strong argument against the occurrence of macroscopic quantum effects in these materials. Quantum tunneling of the phase leads to fluctuating voltage across the junctions which excites the low-energy quasiparticles specific for d -wave junctions, causing decoherence. Contributions to dissipation due to different transport processes, such as channels due to nodal quasiparticles, midgap states, or their combination, have been theoretically identified and distinguished [169–173].

The proof of MQT in d -wave junctions implies that the role of low-energy quasiparticles in creating dissipation is less relevant than expected. This was first proved on GB biepitaxial junctions by the Chalmers–Napoli experiment [41, 42]. The search of macroscopic quantum effects become feasible once high-quality HTS JJs [20] with significant hysteresis in the current-voltage characteristics were available. Hysteresis means significant capacitive effects and a barrier more acting as a dielectric layer, thus supporting SCD measurements.

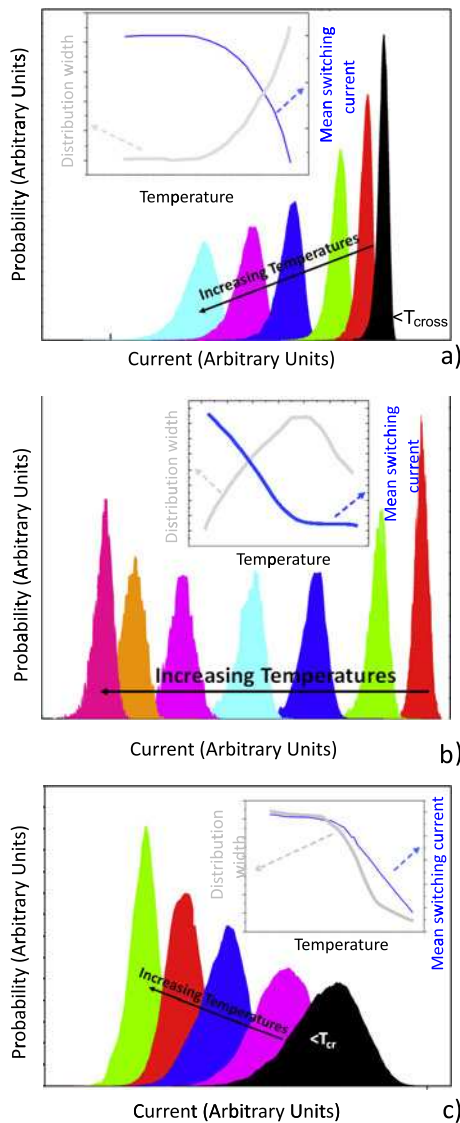


Fig. 2 SCD histograms are schematized in the low (a) and moderate (b) damping regime, respectively. In (c) we are still in the moderate damped regime, but the temperature at which the width σ of the SCD reaches the maximum value T^* is lower than T_{cr} . The temperature dependence of σ and I_{SW} are both reported in the inset of each figure. This behavior is qualitatively quite different providing distinct signatures of the phase dynamics of the various junctions (Color figure on-line)

The GB biepitaxial junctions [35–38] used in [41, 42] had reproducible hysteretic behavior up to 90 %. The tilt configuration (angle $\theta = 0^\circ$) has been selected in order to have the lobe to node configuration, which maximizes *d*-wave induced effects and allows to explore damping also due to low-energy quasiparticles. The SCD as a function of temperature for the biepitaxial JJ substantially follows what commonly measured on LTS JJs, with a saturation of the measured σ below 50 mK [41], which corresponds to the T_{cr} from the thermal to the MQT regime and is consistent with the predicted values. The change of T_{cr} through an external mag-

netic field is an important confirmation of the occurrence of MQT. Values of $R \simeq 100 \Omega$ and $C_J \sim 0.22$ pF can be obtained from the measurements with a plasma frequency $\omega_p/2\pi \simeq 2.6$ GHz and a quality factor of the order of 10 [41, 42, 174]. *C*-axis tilt is mostly responsible for low barrier transparency and leads to the presence of a significant kinetic inductance in the modeling of *YBCO JJ*. In these junctions the presence of a kinetic inductance and a stray capacitance determine the main difference in the washboard potential making the system behavior depending on two degrees of freedom [42, 174–176]. The *YBCO JJ* is coupled to this LC-circuit and the potential becomes two-dimensional (2D).

For *YBCO* biepitaxial junctions engineered on $(La_{0.3}Sr_{0.7})(Al_{0.65}Ta_{0.35})O_3$ (LSAT) substrates [40], a direct transition from phase diffusion (PD) regime to MQT has been demonstrated [43]. These junctions are characterized by higher quality factor $I_c R_N$ and by lower values of capacitance. Since LSAT substrates have a lower dielectric constant with respect to $SrTiO_3$ substrates, this structure allows to isolate GB contribution from stray capacitance, and tends to favor moderately damped regime [40]. The experiment has been designed to meet the condition $T^* < T_{cr}$ taking advantage of the characteristics of these types of junction. At lower temperatures MQT has been observed with the characteristics saturation of σ . Consistently with MQT, the T_{cr} can be tuned by the magnetic field. With increasing temperature there is a direct transition to the PD regime because of the condition $T^* < T_{cr}$. The SCD curves broaden when lowering the *T* and correspondingly the peak intensity decreases [43].

Schematic SCD histograms are reported in Fig. 2c, along with the σ and I_{SW} dependence. The fall off of σ allows an accurate estimations of the dissipation Q , in this case about 1.3, through a fitting procedure based on Monte Carlo simulations [43, 166]. This method is of general utility for all types of junction, in the moderately damped regime where it is not always easy to quantify dissipation through standard technique based on resonant activation measurements [158–160]. Remarkably all parameters are consistently calculated. From the T_{cr} , once known the Q value from the phase diffusion fitting, first $C = 64$ fF and the plasma frequency $\omega_p \simeq 38$ GHz are inferred. This value of the capacitance C is also in agreement with the value extrapolated using the estimated specific capacitance $C_s \simeq 2 \times 10^{-5}$ F cm⁻² for *YBaCuO* BP JJs on LSAT substrates [40]. Similar results have been found in submicron *Nb/AlOx/Nb* [177] and *Al/AlOx/Al* [178] JJs. In Ref. [177] an anomalous $\sigma(T)$ dependence with a negative $d\sigma/dT$ is reported over the entire temperature range. This regime can be achieved by engineering junctions with lower I_c and C , such that the ratio I_c/C , which regulates T_{cr} , is constant and the turn over temperature T^* is lower or comparable to the quantum crossover temperature T_{cr} [158]. In Ref. [178] JJs have

been engineered to obtain low I_c , of about 400 nA, and low capacitance, of about 40 fF, at the same time. In this way TA is completely suppressed since T^* is lower than T_{cr} . On the other hand, by adding a shunting capacitance in the device circuit, TA regime is recovered, showing that the shunting capacitance can be used in order to tune the phase dynamics.

All the junctions considered above fall in the moderately damped junctions ($1 < Q < 10$), and are the obvious consequence of the possibility to reproducibly achieve low I_c in submicron junctions. Lower I_c result in lower Josephson energies E_J , and higher levels of dissipation are expected. The range of the energy dynamical parameters is significantly enlarged, and it is technologically easier to reproducibly realize not trivial configurations. The pioneering studies of Kautz and Martinis [162, 163] and Iansiti et al. [180, 181] on small junctions where E_J could be significantly lowered, can be now supported and developed by different types of junction of quite different sizes. These devices are characterized by intermediate levels of dissipation and by phase diffusion phenomena. The low critical current density J_c limit seems to be characteristic also of all futuristic nano-hybrids devices incorporating nanowires, and the moderately damped regime is intrinsically more common than it could be expected. In this general scenario the experiment in Ref. [43] stands as an example of how it might be relatively easier for HTS junctions to meet the requirement of $T^* < T_{cr}$ and to contribute to settle ($Q, k_B T/E_J$) phase diagram shown in Fig. 3. The transition curve between TA and PD regime has been determined through Monte Carlo simulations, in which the phase dynamics has been explored in a wide range of junction parameters [43, 168, 179]. The good agreement between the transition points shown in Fig. 3, which refer to various works reported in the literature, and the numerically estimated transition curve makes this phase diagram a valid guideline in order to define the relation between E_J , the turn over temperature T^* and the junction quality factor Q . In addition it indicates how the transition from TA to PD regime can be tuned by the critical current and the shunting capacitance of the JJ.

These experiments can be important intermediate steps for the observation of quantum phase diffusion [180, 181]. In the quantum phase diffusion regime E_J and Coulomb energy E_c are expected to be comparable, and quantum effects associated to phase delocalization and classical effects associated to frequency-dependent damping are both determinant [162, 163]. Junctions are underdamped at high frequencies but are in the overdamped limit at low frequencies, respectively.

Another class of experiments on the study of phase dynamics has been realized on $\text{Bi}_2\text{Sr}_2\text{CaCu}_2\text{O}_8$ intrinsic junc-

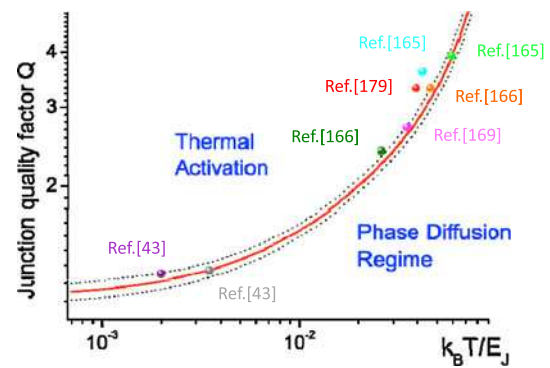


Fig. 3 $Q, k_B T/E_J$ phase diagram. The transition curve between TA and PD regime has been extrapolated through numerical simulations; the sideband curves mark the uncertainty in the calculations and are due to the temperature step size. The points refer to various works reported in the literature in the last ten years. The good agreement between experiments and simulations certifies the universal character of the phase diagram

tions [182, 183]. Interest has been directed to increase the crossover temperature (T_{cr}) and to clarify the nature of IJJs, rather than raising novel themes of coherence in d -wave systems. T_{cr} has been reported to be about 800 mK, remarkably higher than those usually found in LTS systems. By using microwave spectroscopy, the unique uniform array structure of IJJs stacks have been considered responsible for a significant enhancement of the tunneling rate [183]. This enhancement adds a factor of approximately N^2 to the quantum escape rate of a single Josephson junction, also resulting in a significant increase of T_{cr} , where N is the number of the junctions in the stack. This effect can be caused by large quantum fluctuations due to interactions among the N junctions [183].

At the end of this section we present a short list of significant signatures that classify the phase dynamics of a junction and its dissipation, and in particular the transition from TA/MQT to PD regime:

- (1) dependence of width σ of the SCD on the temperature;
- (2) asymmetry of the distribution measured by skewness γ as a function of the temperature that is, the ratio m_3/σ^3 where m_3 is the third central moment of the distribution [43, 166, 168].
- (3) dependence shape of the escape rates Γ on the ratio between the barrier height ΔU and the thermal energy. In TA regime the SCD are asymmetric and skewed to the left, and Γ values all fall onto the same line. Retrapping processes cause a progressive symmetrization of the switching distribution, and a bending in the Γ vs. $\Delta U/k_B T$ [165, 168].

- (4) measurements reported in points 1–3 as a function of magnetic field;
- (5) all junction and characteristic ‘phase dynamics’ parameters need to be estimated and to be self-consistent.

The whole set of data collected in these subsections is a solid framework where most of the phase dynamics can be easily classified through a study of switching current distributions. A phase diagram valid in a large range of dissipation conditions emerges as a functional guide to classify all types of behavior and as a reference for phase dynamics of novel types of junction and system for which the nature of the current-induced transition from the superconducting to the normal state has not been completely clarified.

6 HTS Junctions and Wires on the Meso/Nano Scale

6.1 Submicron Josephson Junctions, Energy Scales and Mesoscopic Effects

Looking at recent literature HTS systems have represented the start for SCD measurements on systems different from LTS junctions. Some of the more recent advances in the field of HTS Josephson devices have been pushed by advances in nanotechnology. Nano-scale junctions get closer to the characteristic scale lengths of HTS (i.e. coherence length, charge domains, ...) and HTS structures (i.e. GB facets, GB dislocation distribution, nano-channel size, ...) and have potentials to isolate intrinsic features and transport regimes of HTS systems. These efforts will lead to understand the ultimate limit of GB performances and to valuable progress in the study of coherence in HTS systems. Looking at the great amount of data available in the literature, to the apparent contrast of several results, or to the fact that some predicted phenomena derived from well-established effects have not yet been clearly detected or only at intermittence (such as 2ϕ component, BTRS, all deriving from d -wave OP symmetry [15, 20]), the only reasonable explanation is to assume that several different tunneling and diffusive processes are active in the transport, but only the morphology of the barrier and of the GB will discriminate the role of each transport mechanism. The microstructure acts as a filter determining additional constraints on the various transport modes, and nano-structures may help to isolate the various contributions. Another relevant issue is that HTS are characterized by scaling lengths and energies quite different from those characteristic of LTS canonical systems. From the fundamental point of view this may lead to novel effects that become observable in experimentally more accessible regimes, while on the applicative side HTS nano-structures can be scaled to much smaller sizes than LTS systems, being superconducting at the same time at much larger temperatures and magnetic fields.

The first studies on bicrystal submicron JJs gave encouraging results as the reduction of decoherence [184], the presence of the 2ϕ component [99], or of Andreev bound states [185, 186]. Recently submicron biepitaxial junctions have been realized down to about 500 nm by using both e-beam lithography and C and Ti masking [46, 187]. Yield and reproducibility have been improved on this width scale, junctions exhibit more uniform barrier and d -wave induced effects are even more controlled [46]. The analysis of the switching process from the superconducting branch to the normal state at voltage value Δ_{sw} has been also carried out, suggesting a correlation of Δ_{sw} with the interface orientation and the d -wave OP profile. The low dissipation of the junctions and a much reduced number of facets have also emerged as characteristic features. These achievements open the way to the ultimate target, i.e., reproducible, single facet junction a few hundreds nanometers wide.

This classical controllable “top-down” approach is accompanied by some sort of “bottom-up” techniques, which fund on the intrinsic nature of GB. The complex growth process may determine self-assembled nano-channels of variable dimensions, ranging typically from 20 nm to 200 nm. These nano-contacts can be considered self-protected as far as they are “enclosed” in macroscopic impurities. Even if this very last technique is not ideal on the long range for applications, since it needs an additional critical step to locate the nanobridges and etch the HTS thin film, it can be really helpful to understand the ultimate limit of the junction performances and to understand the transport mechanisms.

A study on universal conductance fluctuations in magnetic field in YBCO biepitaxial Josephson junctions is an example of how to use the natural self-assembling to investigate relevant issues on HTS JJs such as relaxation processes for quasiparticles [188–190]. The experimental conductance fluctuations as a function of the magnetic field have been studied using autocorrelation function protocols typical of traditional mesoscopic systems. Conductance fluctuations have been measured at low temperatures as a function of magnetic field. The system is in the regime of universal conductance fluctuations, which are nonperiodic, and have all the typical characteristics of mesoscopic fluctuations [191–196].

An energy scale of the order of 1 meV arises naturally from the autocorrelation function that has been identified as the Thouless energy E_{th} [196]. This is proportional to the inverse time an electron spends in moving coherently across the mesoscopic sample. Quasiparticles seem to travel coherently across the junction. Hence, microscopic features of the weak link appear as less relevant, in favor of mesoscopic, non local properties. In this case, the quasiparticle phase coherence time τ_ϕ does not seem to be limited by energy relaxation due to voltage induced non-equilibrium. The remarkably long lifetime of the carriers, found in these

experiments, appears to be a generic property in high- T_C YBCO junctions as proved by optical measurements [197] and by macroscopic quantum tunneling [41, 42]. Magnetoconductance spectra in other words confirm the existence of a characteristic energy scale, revealing nano-channels of size of about 100 nm as paths of the current. Their size defines the characteristic energy of the junction, i.e. the Thouless energy E_{Th} , which is about the $I_C R_N$ value and its direct ‘image’, the minigap E_g , i.e. the gap induced in the barrier region [190]. E_{Th} is quite large when compared to what usually measured in traditional normal metal artificial systems, because the nanocontacts are self-assembled and relatively smaller [190]. E_g in the spectrum is a consequence of the special ‘length-scale hierarchy’ of the device, benefitting of the specific mesoscopic single particle coherence of the sample. These conductance oscillations are expected to be quite general features of mesoscopic junctions as far as the material parameters meet the requirements $\xi_S \ll L \ll L_\phi$ where ξ_S is the coherence length, L the length of the barrier and L_ϕ the phase coherence length, respectively. HTS JJs give access to this regime, which is indeed hardly achievable in LTS proximized structures. Periodical oscillations in the magnetoconductance have been recently measured in proximized gold nanowires up to 1.2 μm long and attributed to the presence of the minigap [198]. The disappearance of those oscillations by changing the length L of the wires confirms that the showing up of the minigap is critical.

These experiments [188–190] not only suggest quasiparticle scattering inefficient in producing relaxation in the Andreev proximity and in reducing the lifetime of the antinodal quasiparticles, but confirm the relevance of possible effective filamentary structures across GBs in the transport modes, as debated also in early times [19, 20, 199–202]. Hints on a more complex vortex dynamics at the GB also come from magnetically imaging the vortices in the GB through scanning area Hall bar microscopy. The voltage across the GB has been inferred from the frequency of the telegraph noise, with voltage sensitivity as small as 2×10^{-16} V, reflecting the motion of millions of vortices across boundary per second [203].

The idea to use the self-protected GB growing in between impurities has been also pursued in [204] by using ‘standard’ e-beam techniques combined to focused ion beam (FIB). By using the competition between the superconducting YBCO and the insulating Y_2BaCuO_5 phases during film growth, nanometer sized GB junctions of the order of 100 nm were formed in the insulating Y_2BaCuO_5 matrix. FIB has been used also to produce nano-SQUIDs employing bicrystal junctions of widths down to 80 nm [205]. Performances are quite promising and respond to the need of sensitive nanoSQUIDs for various applications [206] and in particular for the detection of small spin systems.

One of the next steps to be understood is whether the scale of 100 nm (coming out from the different experiments

discussed above) is representative of the intrinsic nature of HTS or not. A matrix of filaments of smaller size, related to the nature of HTS rather than to the macroscopic artifacts formed during the build-up of the GB, could result for instance from intrinsic stripes [207–209] or from regions where strong correlations are not uniformly distributed along the GB. Charge inhomogeneities at the grain boundary have been also microscopically modeled and identified as a relevant source for the suppression of J_C [210]. A matrix on a scale significantly smaller than 100 nm would have its own fingerprints superimposed on those discussed above.

6.2 HTS Nano-Structures and Nanowires

Junctions obviously benefit of the progress achieved in patterning simple nano-structures and nanowires, not across any engineered GB. Advanced nanolithography techniques have been applied to produce high-quality YBCO nanowires [211–213] down to the scale of 30–50 nm with improved performances and reproducibility when compared with early results [214–219]. An example of a YBCO nanowire, 50 nm wide, realized at NEST in collaboration with University of Napoli is shown in Fig. 4. ‘Standard’ flux-flow I – V curves have been found down to widths of 20–30 nm without any sign of weak-link behavior or of a possible nanotextured structure of HTS. Lack of special fingerprints obviously applies only to standard I – V measurements, since no focused measurements have been realized in absence of clear indications (to our knowledge) of possible benchmarks of a striped structure in I – V curves. The performances of the self-assembled and intrinsically protected junctions contribute to define the ultimate limits of a top-down approach, also in view of possible challenging bottom-up like procedures. In the latter case the film deposition is the last step in the nanofabrication process, and no further chemical or physical treatments are done after the film growth. Top-down and bottom-up nanolithography approaches can both work, even if they are technologically quite complex and advanced. The use of cap layers protecting as long as possible the conducting channel in the fabrication process is functional in preserving the high quality of the original HTS film and GB, and in determining the high quality of the nano-structure. The know-how acquired in dealing with HTS so intrinsically sensitive to processing is a relevant background to keep into account also for producing meso- and nano-structures with novel materials, as for instance pnictide superconductors.

Transport experiments on single nanowires are considered very important to possibly unveil several issues on HTS and its pairing mechanism, to discern various states in the HTS phase diagram by virtue of the system size [217, 218]. This potential of using HTS nano-structures for fundamental

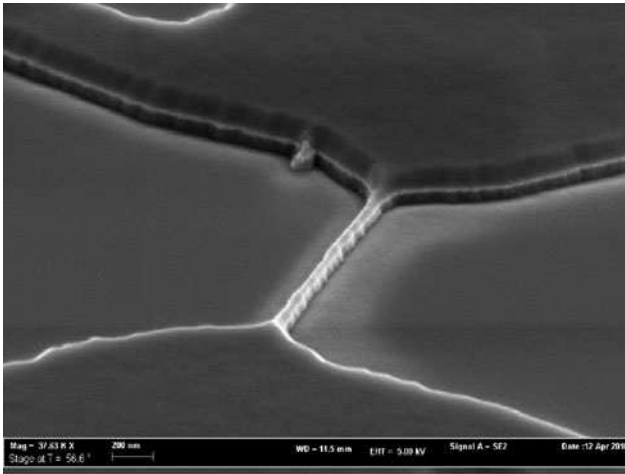


Fig. 4 Scanning Electron Microscope image shows a typical YBCO nanowire realized by E-Beam Lithography fabrication process. The nanowire shown is 1.5 μm long, 50 nm wide and thick. It is covered by a gold cap layer thick 20 nm useful to reduce any damage due the nano-patterning process

topics also extends to curved geometry and non-trivial topology, which is a traditional rich source of novel physics. The properties of single submicron YBCO and LaSrCuO rings have been investigated [220–222], on the boost of claims of a crossover between the typical $h/2e$ superconducting and h/e quasiparticle flux periodicity in mesoscopic loops of length scales even larger than ξ [223–228]. This transition is a manifestation of macroscopic quantum coherence and is favored in an underdoped d -wave system where robust superconductivity along specific directions coexist with low-energy quasiparticles [223–228]. It raises the possibility of manipulation of spin currents (carried by quasiparticles) by controlled motion of magnetic fluxes with applications to spintronics and other areas of applied science.

No such crossover has been observed, but novel insights have been achieved on a concentric vortex structure with nonuniform vorticity (induced by the peculiar HTS relationship between the values of ξ and the London penetration depth) [220] and the interaction between thermally excited moving vortices and the oscillating persistent current induced in the loops [221, 222]. These experiments have been of reference for novel theoretical investigations on mesoscopic rings [229–231]. Large resistance oscillations are due to current-excited moving vortices, where the applied current in competition with the oscillating Meissner currents imposes or removes the barriers for vortex motion [232–235] in an increasing magnetic field [229]. This represents an additional phenomenon to be considered in parallel with the Little–Parks effect in transport measurements, and also with thermal activation of dissipative vortex–antivortex pairs in HTS samples. In [230] it is shown that open superconductor nanotubes provide a tunable generator of superconducting vortices for fluxon-based quantum computing.

All the progress achieved in nanotechnology applied to HTS and in mastering more and more robust and high-quality hetero-structures makes possible the realization of hybrid devices with HTS electrodes incorporating as a tunable barrier nanowires of different materials [236]. This type of architecture not only may benefit of the high temperatures of the electrodes but also of complementary functionalities of the barrier from semiconducting to ferromagnetic. Applications such as field effect transistors [237–239] and nano-sensors may take advantage of these new possibilities offered by nanotechnology. Hybrid nanostructures engineered by inducing superconductivity in semiconducting nanowires with strong spin orbit coupling (e.g. InAs or InSb) by means of nanostructured YBCO leads, can be fruitfully used to display the very elusive Majorana quasiparticles at relatively high temperatures [92]. This would be a great advantage with respect to the very recent experiments involving LTS [240] claiming to see Majorana fermions below 100 mK. Moreover the possibility to engineer HTS (topologically non-trivial) π loops could open novel scenarios for detecting and operating Majorana Fermions with solid state superconducting devices [92].

Nanowires, two-dimensional sheets of induced or intrinsic superconductivity, stripes, clusters potential cells of high critical temperature superconductivity [241, 242] are all the means for new frontiers. From their hybridization with standard bulk superconductors, novel routes towards the secrets of Cooper pairing and of devices of superior performances will be accessible.

6.3 Switching Current Distributions in Nano-Junctions and Nanowires

We conclude this section trying to establish a correlation between nano-structures and escape dynamics. Switching current distribution measurements have been more and more used on a series of different nano-structures. Some of them are junctions and then can be easily classified in the schemes described above, and more specifically in the moderately damped regime. Some of them are simple nanowires. We believe a subtle path exists between these different systems with analogies and quite distinctive features. When considering that a micro-bridge of width of the order of the coherence length behaves as a Josephson junction [4–6], SCD measurements will turn out to be more and more a direct way of discriminating the phase dynamics and the transport in non-trivial cases, which are going to be more and more common with advances in nano-patterning superconductors at extreme scales.

Supercurrent passes in graphene sheets comprised in between superconducting electrodes [243–246]. This is one of the nano-structured proximity-coupled Josephson systems

based on conducting spacers, able in principle to be electrically tuned. Other possibilities other than graphene are offered by nanowires [247, 248], carbon nanotubes [249, 250] and nanocrystals [251]. In [243, 244] graphene is attached to PbIn electrodes separated by a trench of 300 nm. PbIn superconducting electrodes significantly enhances the critical current I_C compared with commonly used Al (as high as 6 μA in highly doped regions). The crossover from the classical to quantum regime is controlled by the gate voltage and has been found surprisingly high of the order of a few hundreds mK. Q factor is about 5–6 for all voltages. Capacitance is for instance about 35 fF at $V = -60$ V and seems to be not related to self-heating [252] but consistent with an effective capacitance $C_{\text{eff}} = \hbar/R_N E_{\text{th}}$ due to diffusive motion of quasiparticles in graphene [253]. Phase diffusion regime has been found for all gate voltages with T^* ranging from about 1 K ($V = 0$ V) to 2 K ($V = -60$ V). Signatures of the Thouless energy [196] and of the minigap, commonly observed in the transport properties of nano-structures should also somehow manifest in the switching dynamics in nano-structures.

Stochastic dynamics of superconductive-resistive switching in hysteretic current-biased superconducting nanowires undergoing phase-slip fluctuations is a topic of growing interest. Recent studies have reported phase-slip induced switching in superconducting nanowires [254–257]. In $\text{Mo}_{79}\text{Ge}_{21}$ nanowires of length ranging from 100 nm up to 200 nm [254], SCD have been used to investigate the behavior of individual quantum phase-slip events at high bias currents, observing a monotonic increase of σ with decreasing temperature. In Al nanowires [255] of width less than 10 nm and length ranging from 1.5 to 10 μm (with critical currents of the order of a few μA), fluctuations in the average critical current exhibit three distinct regions of behavior and are nonmonotonic in temperature. Saturation is present well below the critical temperature T_C , σ increases as $T^{2/3}$ at intermediate temperatures, and a collapse is present close to T_C . The relationship between individual phase slips and switching has been also theoretically investigated [258] in order to provide a tool to study phase slips, to contribute to understand whether they are caused by thermal fluctuations or by macroscopic quantum tunneling [259–266]. It has been found that although several phase-slip events are generally necessary to induce switching, there is an experimentally accessible regime of temperatures and currents for which just one single phase-slip event is sufficient to induce switching, via the local heating it causes.

7 Conclusions

We have revisited some of the most recent advances on the physics of HTS Josephson junctions. The more significant

steps forward in these last years have been made in our opinion towards the fabrication of HTS nano-structures and the study of phase dynamics. These achievements have to be added to the impressive know-how previously acquired in handling experimentally and theoretically problems of significant complexity, due to delicate nature of HTS samples and to the composite physics of HTS. HTS JJs might inspire concepts for the realization of junctions of all novel materials able to address an impressive series of issues. We have focused on macroscopic quantum decay phenomena, as one of the most exciting expressions of the Josephson effect. Switching current distribution measurements are a direct way of discriminating the phase dynamics and the transport also in non-trivial cases of moderate damping, which are going to be more and more common with advances in nano-patterning superconductors and in materials science with novel possibilities of synthesizing also hybrid coplanar systems. A wide vision on macroscopic quantum phenomena in a variety of complementary systems including d -wave junctions can promote novel arguments on the interplay of coherence and dissipation in solid state systems.

Acknowledgements Special thanks to John Kirtley for sharing so many common interests in several experiments reviewed in this manuscript. We would also like to thank Thilo Bauch and Chang Tsuei for valuable discussions on the topics of this contribution. This work is supported by MIUR PRIN 2009 under the project SuFET based on nanowires and HTS. We also acknowledge partial support by STREP Macroscopic Interference Devices for atomic and Solid State Physics: Quantum Control of Supercurrents and by a Marie Curie International Reintegration Grant No. 248933 hybMQC within the 7th European Community Framework Programme.

References

1. Bednorz, J.G., Muller, K.A.: Possible high T_c superconductivity in the Ba–La–Cu–O system. *Z. Phys. B* **64**, 189 (1986)
2. Josephson, B.D.: Possible new effects in superconducting tunnelling. *Phys. Lett.* **1**(7), 251 (1962)
3. Kulik, I.O., Yanson, K.: *The Josephson Effect in Superconductive Tunneling Structures*. Israel Program of Scientific Translations, Jerusalem (1972)
4. Barone, A., Paternó, G.: *Physics and Applications of the Josephson Effect*. Wiley, New York (1982)
5. Likharev, K.K.: *Dynamics of Josephson Junctions and Circuits*. Gordon & Breach, New York (1986)
6. Likharev, K.K.: Superconducting weak links. *Rev. Mod. Phys.* **51**, 101 (1979)
7. Caldeira, A.O., Leggett, A.J.: Influence of dissipation on quantum tunneling in macroscopic systems. *Phys. Rev. Lett.* **46**, 211 (1981)
8. Leggett, A.J.: Prospects in ultralow temperature physics. *J. Phys. (Paris) Colloq.* **39**, C6-1264 (1980)
9. Caldeira, A.O., Leggett, A.J.: Quantum tunneling in a dissipative system. *Ann. Phys. (N.Y.)* **149**, 374 (1983)
10. Andreev, A.F.: Thermal conductivity of the intermediate state of superconductors. *Zh. Eksp. Teor. Fiz.* **46**, 1823 (1964) [*Sov. Phys. JETP* **19**, 1228 (1964)]

11. Kulik, I.O.: Macroscopic quantization and the proximity effect in SNS junctions. *Sov. Phys. JETP* **30**, 944 (1969). *Zh. Eksp. Teor. Fiz.* **30**, 944 (1969)
12. Hu, C.-R.: Midgap surface states as a novel signature for $d_{x^2-y^2}$ -wave superconductivity. *Phys. Rev. Lett.* **72**, 1526 (1994)
13. Kashiwaya, S., Tanaka, Y.: Tunnelling effects on surface bound states in unconventional superconductors. *Rep. Prog. Phys.* **63**, 1641 (2000)
14. Lofwander, T., Shumeiko, V., Wendin, G.: Andreev bound states in high- T_c superconducting junctions. *Supercond. Sci. Technol.* **14**, R53 (2001)
15. Tsuei, C.C., Kirtley, J.R.: Phase-sensitive evidence for d -wave pairing symmetry in electron-doped cuprate superconductors. *Rev. Mod. Phys.* **72**, 969 (2000)
16. Van Harlingen, D.J.: Phase-sensitive tests of the symmetry of the pairing state in the high-temperature superconductors: evidence for $d_{x^2-y^2}$ symmetry. *Rev. Mod. Phys.* **67**, 515 (1995)
17. Van Duzer, T., Turner, C.W.: *Principles of Superconductive Devices and Circuits*. Elsevier, New York (1991)
18. Clarke, J., Wilhelm, F.: Superconducting quantum bits. *Nature* **453**, 1031 (2008)
19. Hilgenkamp, H., Mannhart, J.: Grain boundaries in high- T_c superconductors. *Rev. Mod. Phys.* **74**, 485 (2002)
20. Tafuri, F., Kirtley, J.R.: High T_c superconductor weak links. *Rep. Prog. Phys.* **68**, 2573 (2005)
21. Kirtley, J.R., Tafuri, F.: In: Brooks, J.S., Schrieffer, J.R. (eds.) *Handbook of High-Temperature Superconductivity: Theory and Experiment*, pp. 19–85. Springer, Berlin (2007)
22. Mannhart, J., Chaudhari, P., Dimos, D., Tsuei, C.C., McGuire, T.M.: Critical currents in [001] grains and across their tilt boundaries in $\text{YBa}_2\text{Cu}_3\text{O}_7$ films. *Phys. Rev. Lett.* **61**, 2476 (1988)
23. Chaudari, P., Mannhart, J., Dimos, D., Tsuei, C.C., Chi, C.C., Oprysko, M.M., Scheuermann, M.: Direct measurement of the superconducting properties of single grain boundaries in $\text{Y}_1\text{Ba}_2\text{Cu}_3\text{O}_{7-\delta}$. *Phys. Rev. Lett.* **60**, 1653 (1988)
24. Dimos, D., Chaudhari, P., Mannhart, J.: Superconducting transport properties of grain boundaries in $\text{YBa}_2\text{Cu}_3\text{O}_7$ bicrystals. *Phys. Rev. B* **41**, 4038 (1990)
25. Kamihara, Y., Hiramatsu, H., Hirano, M., Kawamura, R., Yanagi, H., Kamiya, T., Hosono, H.: Iron-based layered superconductor: LaOFeP . *J. Am. Chem. Soc.* **128**, 10012 (2006)
26. Takahashi, H., Igawa, K., Arii, K., Kamihara, Y., Hirano, M., Hosono, H.: Superconductivity at 43 K in an iron-based layered compound $\text{LaO}_{1-x}\text{Fe}_x\text{As}$. *Nature* **453**, 376 (2008)
27. Seidel, P.: Josephson effects in iron based superconductors. *Supercond. Sci. Technol.* **24**, 043001 (2011)
28. Stepantsov, E., Tarasov, M., Naito, M., Tsukada, A., Winkler, D.: Grain boundary weak link in a - b plane in MgB_2 film. *Appl. Phys. Lett.* **89**, 213111 (2006)
29. Nagamatsu, J., Nakagawa, N., Muranaka, T., Zenitani, Y., Akimitsu, J.: Superconductivity at 39 K in magnesium diboride. *Nature* **410**, 63 (2001)
30. Cui, Y., Chen, K., Li, Q., Xi, X.X., Rowell, J.M.: Degradation-free interfaces in MgB_2 /insulator/Pb Josephson tunnel junctions. *Appl. Phys. Lett.* **89**, 202513 (2006)
31. Di Capua, R., Aebersold, H.U., Ferdeghini, C., Ferrando, V., Orgiani, P., Putti, M., Salluzzo, M., Vaglio, R., Xi, X.X.: Role of interband scattering in neutron irradiated MgB_2 thin films by scanning tunneling spectroscopy measurements. *Phys. Rev. B* **75**, 014515 (2007)
32. Iavarone, M., Di Capua, R., Koshelev, A.E., Kwok, W.K., Chiarella, F., Vaglio, R., Kang, W.N., Choi, E.M., Kim, H.J., Lee, S.I., Pogrebnjakov, A.V., Redwing, J.M., Xi, X.X.: Effect of disorder in MgB_2 thin films. *Phys. Rev. B* **71**, 214502 (2005)
33. Rubano, A., Paparo, D., Miletto, F., Scotti di Uccio, U., Marucci, L.: Recombination kinetics of a dense electron-hole plasma in strontium titanate. *Phys. Rev. B* **76**, 125115 (2007)
34. Char, K., Colclough, M.S., Garrison, S.M., Newman, N., Zaharchuk, G.: Biepitaxial grain boundary junctions in $\text{YBa}_2\text{Cu}_3\text{O}_7$. *Appl. Phys. Lett.* **59**, 733 (1991)
35. Tafuri, F., Miletto Granozio, F., Carillo, F., Di Chiara, A., Verbiest, K., Van Tendeloo, G.: Microstructure and Josephson phenomenology in 45° tilt and twist YBaCuO artificial grain boundaries. *Phys. Rev. B* **59**, 11523 (1999)
36. Tafuri, F., Carillo, F., Lombardi, F., Miletto Granozio, F., Ricci, F., Scotti di Uccio, U., Barone, A., Testa, G., Sarnelli, E., Kirtley, J.R.: Feasibility of biepitaxial YBaCuO Josephson junctions for fundamental studies and potential circuit implementation. *Phys. Rev. B* **62**, 14431 (2000)
37. Di Chiara, A., Lombardi, F., Miletto Granozio, F., Scotti di Uccio, U., Tafuri, F., Valentino, M.: YBaCuO grain boundary Josephson junctions with a MgO seed layer. *IEEE Trans. Appl. Supercond.* **7**, 3327 (1997)
38. Lombardi, F., Tafuri, F., Ricci, F., Miletto Granozio, F., Barone, A., Testa, G., Sarnelli, E., Kirtley, J.R., Tsuei, C.C.: Intrinsic d -wave effects in YBaCuO grain boundary Josephson junctions. *Phys. Rev. Lett.* **89**, 207001 (2002)
39. Miletto Granozio, F., Scotti di Uccio, U., Lombardi, F., Ricci, F., Bevilacqua, F., Ausanio, G., Carillo, F., Tafuri, F.: Structure and properties of symmetric and asymmetric YBaCuO Josephson junctions realized by a novel CeO_2 -based biepitaxial technique. *Phys. Rev. B* **67**, 184506 (2003)
40. Stornaiuolo, D., Papari, G., Cennamo, N., Carillo, F., Longobardi, L., Massarotti, D., Barone, A., Tafuri, F.: High quality factor HTS Josephson junctions on low loss substrates. *Supercond. Sci. Technol.* **24**, 045008 (2011)
41. Bauch, T., Lombardi, F., Tafuri, F., Rotoli, G., Barone, A., Delsing, P., Cleason, T.: Macroscopic quantum tunneling in d -wave YBaCuO Josephson junctions. *Phys. Rev. Lett.* **94**, 087003 (2005)
42. Bauch, T., Lindström, T., Tafuri, F., Rotoli, G., Delsing, P., Claesson, T., Lombardi, F.: Quantum dynamics of a d -wave Josephson junction. *Science* **311**, 5757 (2006)
43. Longobardi, L., Massarotti, D., Stornaiuolo, D., Galletti, L., Rotoli, G., Lombardi, F., Tafuri, F.: Direct transition from quantum escape to phase diffusion regime in YBaCuO biepitaxial Josephson junctions. *Phys. Rev. Lett.* **109**, 050601 (2012)
44. Mitchell, E.E., Macfarlane, J.C., Foley, C.P.: Transport properties of variable-angle YBCO step-edge junctions in the a - b plane. *Supercond. Sci. Technol.* **24**, 055004 (2011)
45. Mitchell, E.E., Foley, C.P.: YBCO step-edge junctions: influence of morphology on junction transport. *IEEE Trans. Appl. Supercond.* **21**, 371 (2011)
46. Stornaiuolo, D., Rotoli, G., Cedergren, K., Born, D., Bauch, T., Lombardi, F., Tafuri, F.: Submicron YBaCuO biepitaxial Josephson junctions: d -wave effects and phase dynamics. *J. Appl. Phys.* **107**, 11390 (2010)
47. Ohtomo, A., Hwang, H.Y.: A high-mobility electron gas at the $\text{LaAlO}_3/\text{SrTiO}_3$ heterointerface. *Nature* **427**, 423 (2004)
48. Mannhart, J., Blank, D.H.A., Hwang, H.Y., Millis, A.J., Triscone, J.-M.: Two-dimensional electron gases at oxide interfaces. *Mater. Res. Soc. Bull.* **33**, 1027 (2008)
49. Mannhart, J., Schlom, D.G.: Oxide interfaces—an opportunity for electronics. *Science* **327**, 1607 (2010)
50. Radovic, M., Salluzzo, M., Ristic, Z., Di Capua, R., Lampis, N., Vaglio, R., Miletto Granozio, F.: In situ investigation of the early stage of TiO_2 epitaxy on (001) SrTiO_3 . *J. Chem. Phys.* **135**, 034705 (2011)
51. Antognazza, L., Moeckly, B.H., Geballe, T.H., Char, K.: Properties of high- T_c Josephson junctions with $\text{Y}_{0.7}\text{Ca}_{0.3}\text{Ba}_2\text{Cu}_3\text{O}_{7-\delta}$ barrier layers. *Phys. Rev. B* **52**, 4559 (1995)

52. Gurvitch, M., Valles, J.J.M., Cucolo, A.M., Dynes, R.C., Garmo, J.P., Schneemeyer, L.F., Waszcak, J.V.: Reproducible tunneling data on chemically etched single crystals of $\text{YBa}_2\text{Cu}_3\text{O}_7$. *Phys. Rev. Lett.* **63**, 1008 (1989)
53. Wollman, D.A., Van Harlingen, D.J., Lee, W.C., Ginsberg, D.M., Leggett, A.J.: Experimental determination of the superconducting pairing state in YBCO from the phase coherence of YBCO-Pb dc SQUIDS. *Phys. Rev. Lett.* **71**, 2134 (1993)
54. Wollman, D.A., Van Harlingen, D.J., Giapintzakis, J., Ginsberg, D.M.: Evidence for $d_{x^2-y^2}$ pairing from the magnetic field modulation of $\text{YBa}_2\text{Cu}_3\text{O}_7$ -Pb Josephson junctions. *Phys. Rev. Lett.* **74**, 797 (1995)
55. Katz, A.G., Sun, A.G., Dynes, R.C., Char, K.: Fabrication of all thin-film $\text{YBa}_2\text{Cu}_3\text{O}_7 - \delta/\text{Pb}$ Josephson tunnel junctions. *Appl. Phys. Lett.* **66**, 105 (1995)
56. Smilde, H.J.H., Ariando, D.H., Blank, A., Gerritsma, G.J., Hilgenkamp, H., Rogalla, H.: d -wave induced Josephson current counterflow in $\text{YBa}_2\text{Cu}_3\text{O}_7/\text{Nb}$ zigzag junctions. *Phys. Rev. Lett.* **88**, 057004 (2002)
57. Bozovic, I., Logvenov, G., Verhoeven, M.A.J., Caputo, P., Goldobin, E., Geballe, T.H.: No mixing of superconductivity and antiferromagnetism in a high-temperature superconductor. *Nature* **422**, 873 (2003)
58. Virshup, G.F., Klusmeier-Brown, M.E., Bozovic, I., Eckstein, J.N.: Hysteretic, high T_c Josephson junctions using heterostructure trilayer films grown by molecular beam epitaxy. *Appl. Phys. Lett.* **60**, 2288 (1992)
59. Klusmeier-Brown, M.E., Virshup, G.F., Bozovic, I., Eckstein, J.N., Ralls, K.S.: Engineering of ultrathin barriers in high T_c , trilayer Josephson junctions. *Appl. Phys. Lett.* **60**, 2806 (1992)
60. Bozovic, I., Logvenov, G., Verhoeven, M.A.J., Caputo, P., Goldobin, E., Beasley, M.R.: Giant proximity effect in cuprate superconductors. *Phys. Rev. Lett.* **93**, 157002 (2004)
61. Demler, E., Berlinsky, A.J., Kallin, C., Arnold, G.B., Beasley, M.R.: Proximity effect and Josephson coupling in the $\text{SO}(5)$ theory of high- T_c superconductivity. *Phys. Rev. Lett.* **80**, 2917 (1998)
62. den Hartog, B.C., Berlinsky, A.J., Kallin, C.: Properties of superconductor–antiferromagnet–superconductor Josephson junctions in $\text{SO}(5)$ theory. *Phys. Rev. B* **59**, R11645 (1999)
63. Decca, R.S., Drew, H.D., Osquiguil, E., Maiorov, B., Guimpel, J.: Anomalous proximity effect in underdoped $\text{YBa}_2\text{Cu}_3\text{O}_{6+x}$ Josephson junctions. *Phys. Rev. Lett.* **85**, 3708 (2000)
64. Kresin, V., Ovchinnikov, Yu., Wolf, S.: Giant Josephson proximity effect. *Appl. Phys. Lett.* **83**, 722 (2003)
65. Kleiner, R., Stenmeyer, F., Kunkel, G., Muller, P.: Intrinsic Josephson effects in $\text{Bi}_2\text{Sr}_2\text{CaCu}_2\text{O}_8$ single crystals. *Phys. Rev. Lett.* **68**, 2394 (1992)
66. Kleiner, R., Muller, P.: Intrinsic Josephson effects in high- T_c superconductors. *Phys. Rev. B* **49**, 1327 (1994)
67. Yurgens, A.A.: Intrinsic Josephson junctions: recent developments. *Supercond. Sci. Technol.* **13**, R85 (2000)
68. Wang, H.B., Wu, P.H., Yamashita, T.: Stacks of intrinsic Josephson junctions singled out from inside $\text{Bi}_2\text{Sr}_2\text{CaCu}_2\text{O}_{8+x}$ single crystals. *Appl. Phys. Lett.* **78**, 4010 (2001)
69. Krasnov, V.M., Golod, T., Bauch, T., Delsing, P.: Anticorrelation between temperature and fluctuations of the switching current in moderately damped Josephson junctions. *Phys. Rev. B* **76**, 224517 (2007)
70. Krasnov, V.M., Bauch, T., Intiso, S., Hurfeld, E., Akazaki, T., Takayanagi, H., Delsing, P.: Collapse of thermal activation in moderately damped Josephson junctions. *Phys. Rev. Lett.* **95**, 157002 (2005)
71. Tsuei, C.C., Kirtley, J.R., Chi, C.C., Yu-Jahnes, L.S., Gupta, A., Shaw, T., Sun, J.Z., Ketchen, M.B.: Pairing symmetry and flux quantization in a tricrystal superconducting ring of $\text{YBa}_2\text{Cu}_3\text{O}_{7-\delta}$. *Phys. Rev. Lett.* **73**, 593 (1994)
72. Ryazanov, V.V., Oboznov, V.A., Veretennikov, A.V., Rusanov, A.Yu.: Intrinsically frustrated superconducting array of superconductor-ferromagnet-superconductor π junctions. *Phys. Rev. B* **65**, 020501(R) (2001)
73. Bauer, A., Bentner, J., Aprili, M., Della Rocca, M.L., Reinwald, M., Wegscheider, W., Strunk, C.: Spontaneous supercurrent induced by ferromagnetic π junctions. *Phys. Rev. Lett.* **92**, 217001 (2004)
74. Buzdin, A.I.: Proximity effects in superconductor-ferromagnet heterostructures. *Rev. Mod. Phys.* **77**, 935976 (2005)
75. Khaire, T.S., Khasawneh, M.A., Pratt, W.P., Birge, N.O.: Observation of spin-triplet superconductivity in Co-based Josephson junctions. *Phys. Rev. Lett.* **104**, 137002 (2010)
76. Kawabata, S., Asano, Y., Tanaka, Y., Golubov, A.A., Kashiwaya, S.: Josephson π state in a ferromagnetic insulator. *Phys. Rev. Lett.* **104**, 117002 (2010)
77. Senapati, K., Blamire, M.G., Barber, Z.H.: Spin-filter Josephson junctions. *Nat. Mater.* **10**, 849 (2011)
78. Walker, M.B., Luettmmer-Strathman, J.: Josephson tunneling in high- T_c superconductors. *Phys. Rev. B* **54**, 588 (1996)
79. Sigrist, M., Rice, T.M.: Paramagnetic effect in high T_c superconductors—a hint for d -wave superconductivity. *J. Phys. Soc. Jpn.* **61**, 4283 (1992)
80. Hilgenkamp, H.: π -phase shift Josephson structures. *Supercond. Sci. Technol.* **21**, 034011 (2008)
81. Sigrist, M.: Time-reversal symmetry breaking states in high-temperature superconductors. *Prog. Theor. Phys.* **99**, 899 (1998)
82. Goldobin, E., Koelle, D., Kleiner, R., Buzdin, A.: Josephson junctions with second harmonic in the current-phase relation: properties of ϕ junctions. *Phys. Rev. B* **76**, 224523 (2007)
83. Fu, L., Kane, C.L., Mele, E.J.: Superconducting proximity effect and Majorana fermions at the surface of a topological insulator. *Phys. Rev. Lett.* **100**, 096407 (2008)
84. Fu, L., Kane, C.L.: Josephson current and noise at a superconductor/quantum-spin-Hall-insulator/superconductor junction. *Phys. Rev. B* **79**, 161408(R) (2009)
85. Tanaka, Y., Yokoyama, T., Nagaosa, N.: Manipulation of the Majorana fermion, Andreev reflection, and Josephson current on topological insulators. *Phys. Rev. Lett.* **103**, 107002 (2009)
86. Lutchyn, R.M., Sau, J.D., Das Sarma, S.: Majorana fermions and a topological phase transition in semiconductor–superconductor heterostructures. *Phys. Rev. Lett.* **105**, 077001 (2010)
87. Akhmerov, A.R., Nilsson, J., Beenakker, C.W.J.: Electrically detected interferometry of majorana fermions in a topological insulator. *Phys. Rev. Lett.* **102**, 216404 (2009)
88. Pablo, S.-J., Prada, E., Aguado, R.: A Josephson effect in finite-length nanowire junctions with Majorana modes. *Phys. Rev. Lett.* **108**, 257001 (2012)
89. Veldhorst, M., Molenaar, C.G., Wang, X.L., Hilgenkamp, H., Brinkman, A.: Experimental realization of superconducting quantum interference devices with topological insulator junctions. *Appl. Phys. Lett.* **100**, 072602 (2012)
90. Veldhorst, M., Snelder, M., Hoek, M., Gang, T., Wang, X.L., Guduru, V.K., Zeitler, U., Wiel, W.G., Golubov, A.A., Hilgenkamp, H., Brinkman, A.: Josephson supercurrent through a topological insulator surface state. *Nat. Mater.* **11**, 417 (2012)
91. Williams, J.R., Bestwick, A.J., Gallagher, P., Hong, S.S., Cui, Y., Bleich, A.S., Analytis, J.G., Fisher, I.R., Goldhaber-Gordon, D.: Unconventional Josephson effect in hybrid superconductor-topological insulator devices. *Phys. Rev. Lett.* **109**, 056803 (2012)
92. Lucignano, P., Mezzacapo, A., Tafuri, F., Tagliacozzo, A.: Advantages of using YBCO-nanowire-YBCO heterostructures in the search for Majorana fermions. *Phys. Rev. B* **86**, 144513 (2012)

93. Takei, S., Fregoso, B.M., Galitski, V., Das Sarma, S.: Topological superconductivity and Majorana fermions in hybrid structures involving cuprate high- T_c superconductors. *Cond. Mat.* **1206.3226** (2012)
94. Yamakage, A., Sato, M., Kashiwaya, S., Tanaka, Y.: Anomalous Josephson current in superconducting topological insulator. *Cond. Mat.* **1208.5306** (2012)
95. Golubov, A.A., Kupryanov, M.Yu., Ilichev, E.: The current-phase relation in Josephson junctions. *Rev. Mod. Phys.* **76**, 411 (2004)
96. Kulik, I.O., Omelyanchuk, A.N.: Contribution to the microscopic theory of the Josephson effect in superconducting bridges. *Pis'ma Zh. Eksp. Teor. Fiz.* **21**, 216 (2005) [*JETP Lett.* **21**, 96 (2005)]
97. Kulik, I.O., Omelyanchuk, A.N.: Properties of superconducting microbridges in the pure limit. *Fiz. Nizk. Temp.* **4**, 945 (1977) [*Sov. J. Low Temp. Phys.* **3**, 459 (1977)]
98. Ilichev, E., Zakosarenko, V., Ljsselsteijn, R.P.J., Hoenig, H.E., Schultze, V., Meyer, H.G., Grajcar, M., Hlubina, R.: Anomalous periodicity of the current-phase relationship of grain-boundary Josephson junctions in high- T_c superconductors. *Phys. Rev. B* **60**, 3096 (1999)
99. Ilichev, E., Grajcar, M., Hlubina, R., Ljsselsteijn, R.P.J., Hoenig, H.E., Meyer, H.G., Golubov, A., Amin, M.H.S., Zagoskin, A.M., Omelyanchuk, A.N., Kupriyanov, M.Yu.: Degenerate ground state in a mesoscopic $\text{YBa}_2\text{Cu}_3\text{O}_{7-x}$ grain boundary Josephson junction. *Phys. Rev. Lett.* **86**, 5369 (2001)
100. Lindström, T., Charlebois, S.A., Tzalenchuk, A.Ya., Ivanov, Z., Amin, M.H.S., Zagoskin, A.M.: Dynamical effects of an unconventional current-phase relation in YBCO dc SQUIDS. *Phys. Rev. Lett.* **90**, 117002 (2003)
101. Gardiner, C.H., Lee, R.A.M., Gallop, J.C., Tzalenchuk, A.Ya., Macfarlane, J.C., Hao, L.: Degenerate ground state and anomalous flux hysteresis in an $\text{YBa}_2\text{Cu}_3\text{O}_7$ grain boundary rf SQUID. *Supercond. Sci. Technol.* **17**, S234 (2004)
102. Terpstra, D., IJsselsteijn, R.P.J., Rogalla, H.: Subharmonic Shapiro steps in high- T_c Josephson junctions. *Appl. Phys. Lett.* **66**, 2286 (1995)
103. Early, E.A., Clark, A.F., Char, K.: Half integral constant voltage steps in high- T_c grain boundary junctions. *Appl. Phys. Lett.* **62**, 3357 (1993)
104. Bulaevskii, L.N., Kuzii, V.V., Sobyani, A.A.: Superconducting system with weak coupling to the current in the ground state. *JETP Lett.* **25**, 290 (1977)
105. Geshkenbein, V.B., Larkin, A.I.: The Josephson effect in superconductors with heavy fermions. *JETP Lett.* **43**(6), 395 (1986)
106. Geshkenbein, V.B., Larkin, A.I., Barone, A.: Vortices with half magnetic flux quanta in heavy-fermion superconductors. *Phys. Rev. B* **36**, 235 (1987)
107. Braunisch, W., Knauf, N., Kateev, V., Neuhausen, S., Grütz, A., Kock, A., Roden, B., Khomskii, D., Wohlleben, D.: Paramagnetic Meissner effect in Bi high temperature superconductors. *Phys. Rev. Lett.* **68**, 1908 (1992)
108. Andreev, A.V., Buzdin, A.I., Osgood, R.M.: π phase in magnetic-layered superconductors. *Phys. Rev. B* **43**, 10124 (1991)
109. Goldobin, E., Koelle, D., Kleiner, R.: Semifluxons in long Josephson $0-\pi$ junctions. *Phys. Rev. B* **66**, 100508(R) (2002)
110. Goldobin, E., Koelle, D., Kleiner, R.: Ground states of one and two fractional vortices in long Josephson $0-k$ junctions. *Phys. Rev. B* **70**, 174519 (2004)
111. Schulz, R.R., Chesca, B., Goetz, B., Schneider, C.W., Schmehl, A., Bielefeldt, H., Hilgenkamp, H., Mannhart, J., Tsuei, C.C.: Design and realization of an all d -wave dc π -superconducting quantum interference device. *Appl. Phys. Lett.* **76**, 912 (2000)
112. Hilgenkamp, H.J.H., Ariando, Smilde, H., Blank, D.H.A., Rijnders, G., Rogalla, H., Kirtley, J.R., Tsuei, C.C.: Ordering and manipulation of the magnetic moments in large-scale superconducting π -loop arrays. *Nature* **422**, 50 (2003)
113. Kirtley, J.R., Tsuei, C.C., Ariando, Verwijs, C.J.M., Harkema, S., Hilgenkamp, H.: Angle-resolved phase-sensitive determination of the in-plane gap symmetry in YBCO. *Nat. Phys.* **2**, 190 (2006)
114. Kirtley, J.: Fundamental studies of superconductors using scanning magnetic imaging. *Rep. Prog. Phys.* **73**, 126501 (2010)
115. Bjornsson, P.G., Maeno, Y., Huber, M.E., Moler, K.: Scanning magnetic imaging of Sr_2RuO_4 . *Phys. Rev. B* **72**, 12504 (2005)
116. Kirtley, J.R., Kallin, C., Hicks, C.W., Kim, E.A., Liu, Y., Moler, K.A., Maeno, Y.Y., Nelson, K.D.: Upper limit on spontaneous supercurrents in Sr_2RuO_4 . *Phys. Rev. B* **76**, 14526 (2007)
117. Hicks, C.W., Kirtley, J.R., Lippman, T.M., Koshnick, N.C., Huber, M.E., Maeno, Y., Yuhasz, W.M., Maple, M.B., Moler, K.A.: Limits on superconductivity-related magnetization in Sr_2RuO_4 and $\text{PrOs}_4\text{Sb}_{12}$ from scanning SQUID microscopy. *Phys. Rev. B* **81**, 214501 (2010)
118. Maeno, Y., Hashimoto, H., Yoshida, K., Nishizaki, S., Fujita, T., Bednorz, J.G., Lichtenberg, F.: Superconductivity in a layered perovskite without copper. *Nature* **372**, 532 (1994)
119. Mackenzie, A.P., Maeno, Y.: The superconductivity of Sr_2RuO_4 and the physics of spin-triplet pairing. *Rev. Mod. Phys.* **75**, 657–712 (2003)
120. Fittipaldi, R., Vecchione, A., Ciancio, R., Pace, S., Cuoco, M., Stornaiuolo, D., Born, D., Tafuri, F., Olsson, E., Kittaka, S., Yaguchi, H., Maeno, Y.: Superconductivity in Sr_2RuO_4 - $\text{Sr}_3\text{Ru}_2\text{O}_7$ eutectic crystals. *Europhys. Lett.* **83**, 27007 (2008)
121. Tafuri, F., Kirtley, J.R., Medaglia, P.G., Orgiani, P., Balestrino, G.: Penetration depths of artificially layered $[\text{Ba}_{0.9}\text{Nd}_{0.1}\text{CuO}_{2+x}]_m/[\text{CaCuO}_2]_n$ systems. *Phys. Rev. Lett.* **92**, 157006 (2004)
122. Bert, J.A., Kalisky, B., Bell, C., Kim, M., Hikita, Y., Hwang, H.Y., Moler, K.A.: Direct imaging of the coexistence of ferromagnetism and superconductivity at the $\text{LaAlO}_3/\text{SrTiO}_3$ interface. *Nat. Phys.* **7**, 767 (2011)
123. Kalisky, B., Kirtley, J.R., Analytis, J.G., Chu, J.-H., Vailionis, A., Fisher, I.R., Moler, K.A.: Stripes of increased diamagnetic susceptibility in underdoped superconducting $\text{Ba}(\text{Fe}_{1-x}\text{Co}_x)_2\text{As}_2$ single crystals: evidence for an enhanced superfluid density at twin boundaries. *Phys. Rev. B* **81**, 184513 (2010)
124. Smilde, H.J.H., Golubov, A.A., Ariando, Rijnders, G., Dekkers, J.M., Harkema, S., Blank, D.H.A., Rogalla, H., Hilgenkamp, H.: Admixtures to d -wave gap symmetry in untwinned YBaCuO superconducting films measured by angle-resolved electron tunneling. *Phys. Rev. Lett.* **95**, 257001 (2005)
125. Dekkers, J.M., Rijnders, G., Harkema, S., Smilde, H.J.H., Hilgenkamp, H., Rogalla, H., Blank, D.H.A.: Monocrystalline YBaCuO thin films on vicinal SrTiO (001) substrates. *Appl. Phys. Lett.* **83**, 5199 (2003)
126. Gustafsson, D., Golubev, D., Fogelstrom, M., Claeson, T., Bauch, T., Lombardi, F.: Fully gapped superconductivity in a nanometer size YBaCuO island enhanced by magnetic field. Unpublished (2012)
127. Copetti, C.A., Ruders, F., Oelze, B., Buchal, Ch., Kabius, B., Seo, J.W.: Electrical properties of 45° grain boundaries of epitaxial YBaCuO , dominated by crystalline microstructure and d -wave-symmetry. *Physica C* **253**, 63 (1995)
128. Mannhart, J., Hilgenkamp, H., Mayer, B., Gerber, Ch., Kirtley, J.R., Moler, K.A., Sigrist, M.: Generation of magnetic flux by single grain boundaries of YBaCuO . *Phys. Rev. Lett.* **77**, 2782 (1996)
129. Hilgenkamp, H., Mannhart, J., Mayer, B.: Implications of $d_{x^2-y^2}$ symmetry and faceting for the transport properties of grain

- boundaries in high- T_c superconductors. *Phys. Rev. B* **53**, 14586 (1996)
130. Kirtley, J.R., Chaudhari, P., Ketchen, M.B., Khare, N., Lin, S.-Y., Shaw, T.: Distribution of magnetic flux in high- T_c grain-boundary junctions enclosing hexagonal and triangular areas. *Phys. Rev. B* **51**, R12057 (1995)
 131. Tafuri, F., Kirtley, J.R., Lombardi, F., Miletto Granozio, F.: Intrinsic and extrinsic d -wave effects in YBaCuO grain boundary Josephson junctions: implications for π -circuitry. *Phys. Rev. B* **67**, 174516 (2003)
 132. Mints, R.G., Papiashvili, I., Kirtley, J.R., Hilgenkamp, H., Hammerl, G., Mannhart, J.: Observation of splintered Josephson vortices at grain boundaries in YBaCuO. *Phys. Rev. Lett.* **89**, 067004 (2002)
 133. Mints, R.G., Papiashvili, I.: Josephson vortices with fractional flux quanta at YBa₂Cu₃O_{7-x} grain boundaries. *Phys. Rev. B* **64**, 134501 (2001)
 134. Amin, M.H.S., Omelyanchouk, A.N., Zagoskin, A.M.: Mechanisms of spontaneous current generation in an inhomogeneous d -wave superconductor. *Phys. Rev. B* **63**, 212502 (2001)
 135. Amin, M.H.S., Rashkeev, S.N., Coury, M., Omelyanchouk, A.N., Zagoskin, A.M.: $d+is$ versus $d+id$ time reversal symmetry breaking states in finite size systems. *Phys. Rev. B* **66**, 174515 (2002)
 136. Sigrist, M., Bailey, D.B., Laughlin, R.B.: Fractional vortices as evidence of time-reversal symmetry breaking in high-temperature superconductors. *Phys. Rev. Lett.* **74**, 3249 (1995)
 137. Bailey, D.B., Sigrist, M., Laughlin, R.B.: Fractional vortices on grain boundaries: the case for broken time-reversal symmetry in high-temperature superconductors. *Phys. Rev. B* **55**, 15239 (1997)
 138. Lofwander, T., Shumeiko, V.S., Wendin, G.: Time-reversal symmetry breaking at Josephson tunnel junctions of purely d -wave superconductors. *Phys. Rev. B* **62**, R14653 (2000)
 139. Carmi, R., Polturak, E., Koren, G., Auerbach, A.: Spontaneous macroscopic magnetization at the superconducting transition temperature of YBaCuO7. *Nature* **404**, 853 (2000)
 140. Tafuri, F., Kirtley, J.R.: Spontaneous magnetic moments in YBaCuO thin films. *Phys. Rev. B* **62**, 13934 (2000)
 141. Kosterlitz, J.M., Thouless, D.J.: Ordering, metastability and phase transitions in two-dimensional systems. *J. Phys. C* **6**, 1181 (1973)
 142. Kirtley, J.R., Tsuei, C.C., Tafuri, F.: Thermally activated spontaneous fluxoid formation in superconducting thin film rings. *Phys. Rev. Lett.* **90**, 257001 (2003)
 143. Zasadzinski, J.: In: Bennemann, K.H., Ketterson, J.B. (eds.) *The Physics of Superconductors*, vol. I, p. 591. Springer, Berlin (2003)
 144. Covington, M., Aprili, M., Paraoanu, E., Greene, L.H., Xu, F., Zhu, J., Mirkin, C.A.: Observation of surface-induced broken time-reversal symmetry in YBaCuO tunnel junctions. *Phys. Rev. Lett.* **79**, 277 (1997)
 145. Fogelstrom, M., Rainer, D., Sauls, J.A.: Tunneling into current-carrying surface states of high- T_c superconductors. *Phys. Rev. Lett.* **79**, 281 (1997)
 146. Aprili, M., Covington, M., Paraoanu, E., Niedermeier, B., Greene, L.H.: Tunneling spectroscopy of the quasiparticle Andreev bound state in ion-irradiated YBaCuO/Pb junctions. *Phys. Rev. B* **57**, R8139 (1998)
 147. Tomaschko, J., Scharinger, S., Leca, V., Nagel, J., Kemmler, M., Selistrowski, T., Koelle, D., Kleiner, R.: Phase-sensitive evidence for $d_{x^2-y^2}$ -pairing symmetry in the parent-structure high- T_c cuprate superconductor Sr_{1-x}La_xCuO₂. *Phys. Rev. B* **86**, 094509 (2012)
 148. Kramers, H.A.: Brownian motion in a field of force and the diffusion model of chemical reactions. *Physica (Utrecht)* **7**, 284 (1940)
 149. Ivanchenko, Yu.M., Zilberman, L.A.: The Josephson effect on small size tunnel contacts. *Zh. Èksp. Teor. Fiz.* **55**, 2396 (1968) [*Sov. Phys. JETP* **28**, 1272 (1969)]
 150. Voss, R.F., Webb, R.A.: Macroscopic quantum tunneling in 1- μ m Nb Josephson junctions. *Phys. Rev. Lett.* **47**, 265 (1981)
 151. Jackel, L.D., Gordon, J.P., Hu, E.L., Howard, R.E., Fetter, L.A., Tennant, D.M., Epworth, R.W., Kurkijarvi, J.: Decay of the zero-voltage state in small-area, high-current-density Josephson junctions. *Phys. Rev. Lett.* **47**, 697 (1981)
 152. der Boer, W., de Bruyn Ouboter, R.: Flux transition mechanisms in superconducting loops closed with a low capacitance point contact. *Physica B* **98**, 185 (1980)
 153. Bol, D.W., Scheffer, J.J.F., Giele, W., de Bruyn Ouboter, R.: Thermal activation in the quantum regime and macroscopic quantum tunnelling in the thermal regime in a metastable system consisting of a superconducting ring interrupted by a weak junction, part I: thermal activation in the quantum regime. *Physica B* **113**, 196 (1985)
 154. Prance, R.J., Long, A.P., Clarke, T.D., Widom, A., Mutton, J.E., Sacco, J., Potts, M.W., Negaloudis, G., Goodall, F.: Macroscopic quantum electrodynamic effects in a superconducting ring containing a Josephson weak link. *Nature* **289**, 543 (1981)
 155. Dimitrenko, I.M., Khlus, V.A., Tsoi, G.M., Shnyrkov, V.I.: Quantum decay of metastable current states in rf SQUIDS. *Fiz. Nizk. Temp.* **11**, 146 (1985) [*Sov. J. Low Temp. Phys.* **11**, 77 (1985)]
 156. Washburn, S., Webb, R.A., Voss, R.F., Farris, S.M.: Effects of dissipation and temperature on macroscopic quantum tunneling. *Phys. Rev. Lett.* **54**, 2712 (1985)
 157. Schartz, D.B., Sen, B., Archie, C.N., Lukens, J.E.: Quantitative study of the effect of the environment on macroscopic quantum tunneling. *Phys. Rev. Lett.* **55**, 1547 (1985)
 158. Devoret, M.H., Martinis, J.M., Clarke, J.: Measurements of macroscopic quantum tunneling out of the zero-voltage state of a current-biased Josephson junction. *Phys. Rev. Lett.* **55**, 1908 (1985)
 159. Martinis, J.M., Devoret, M.H., Clarke, J.: Experimental tests for the quantum behavior of a macroscopic degree of freedom: the phase difference across a Josephson junction. *Phys. Rev. B* **35**, 4682 (1987)
 160. Martinis, J.M., Devoret, M.H., Clarke, J.: Energy-level quantization in the zero-voltage state of a current-biased Josephson junction. *Phys. Rev. Lett.* **55**, 1543 (1985)
 161. Fulton, T.A., Dunkleberger, L.N.: Lifetime of the zero-voltage state in Josephson tunnel junctions. *Phys. Rev. B* **9**, 4760 (1974)
 162. Kautz, R.L., Martinis, J.M.: Noise-affected I-V curves in small hysteretic Josephson junctions. *Phys. Rev. B* **42**, 9903 (1990)
 163. Martinis, J.M., Kautz, R.L.: Classical phase diffusion in small hysteretic Josephson junctions. *Phys. Rev. Lett.* **63**, 1507 (1989)
 164. Kivioja, J.M., Nieminen, T.E., Claudon, J., Buisson, O., Hekking, F.W.J., Pekola, J.P.: Observation of transition from escape dynamics to underdamped phase diffusion in a Josephson junction. *Phys. Rev. Lett.* **94**, 247002 (2005)
 165. Männik, J., Li, S., Qiu, W., Chen, W., Patel, V., Han, S., Lukens, J.E.: Crossover from Kramers to phase-diffusion switching in moderately damped Josephson junctions. *Phys. Rev. B* **71**, 220509 (2005)
 166. Fenton, J.C., Warburton, P.A.: Monte Carlo simulations of thermal fluctuations in moderately damped Josephson junctions: multiple escape and retrapping, switching- and return-current distributions, and hysteresis. *Phys. Rev. B* **78**, 054526 (2008)
 167. Longobardi, L., Massarotti, D., Rotoli, G., Stornaiuolo, D., Papari, G., Kawakami, A., Pepe, G.P., Barone, A., Tafuri, F.: Quantum crossover in moderately damped epitaxial NbN/MgO/NbN junctions with low critical current density. *Appl. Phys. Lett.* **99**, 062510 (2011)

168. Longobardi, L., Massarotti, D., Rotoli, G., Stornaiuolo, D., Pappari, G., Kawakami, A., Pepe, G.P., Barone, A., Tafuri, F.: Thermal hopping and retrapping of a Brownian particle in the tilted periodic potential of a NbN/MgO/NbN Josephson junction. *Phys. Rev. B* **84**, 184504 (2011)
169. Fominov, Y.V., Golubov, A.A., Kupriyanov, M.Y.: Decoherence due to nodal quasiparticles in *d*-wave qubits. *JETP Lett.* **77**, 587 (2003)
170. Amin, M.H.S., Smirnov, A.Y.: Quasiparticle decoherence in *d*-wave superconducting qubits. *Phys. Rev. Lett.* **92**, 017001 (2004)
171. Kawabata, S., Kashiwaya, S., Asano, Y., Tanaka, Y.: Macroscopic quantum tunneling and quasiparticle dissipation in *d*-wave superconductor Josephson junctions. *Phys. Rev. B* **70**, 132505 (2004)
172. Kawabata, S., Kashiwaya, S., Asano, Y., Tanaka, Y.: Effect of zero-energy bound states on macroscopic quantum tunneling in high- T_c superconductor junctions. *Phys. Rev. B* **72**, 052506 (2005)
173. Yokoyama, T., Kawabata, S., Kato, T., Tanaka, Y.: Theory of macroscopic quantum tunneling in high- T_c *c*-axis Josephson junctions. *Phys. Rev. B* **76**, 134501 (2007)
174. Rotoli, G., Bauch, T., Lindstrom, T., Stornaiuolo, D., Tafuri, F., Lombardi, F.: Classical resonant activation of a Josephson junction embedded in an LC circuit. *Phys. Rev. B* **75**, 144501 (2007)
175. Kawabata, S., Bauch, T., Kato, T.: Theory of two-dimensional macroscopic quantum tunneling in $\text{YBa}_2\text{Cu}_3\text{O}_{7-x}$ Josephson junctions coupled to an LC circuit. *Phys. Rev. B* **80**, 174513 (2009)
176. Claeson, T., Lombardi, F., Bauch, T., Lindström, T., Barone, P.D.A., Tafuri, F., Rotoli, G.: Macroscopic quantum phenomena in high critical temperature superconducting Josephson junctions. *J. Supercond. Nov. Magn.* **19**, 341 (2006)
177. Yu, H.F., Zhu, X.B., Peng, Z.H., Tian, Ye, Cui, D.J., Chen, G.H., Zheng, D.N., Jing, X.N., Lu, L., Zhao, S.P., Han, S.: Quantum phase diffusion in a small underdamped Josephson junction. *Phys. Rev. Lett.* **107**, 067004 (2011)
178. Yoon, Y., Gasparinetti, S., Mottonen, M., Pekola, J.P.: Capacitively enhanced thermal escape in underdamped Josephson junctions. *J. Low Temp. Phys.* **163**, 164 (2011)
179. Massarotti, D., Longobardi, L., Galletti, L., Stornaiuolo, D., Montemurro, D., Pepe, G., Rotoli, G., Barone, A., Tafuri, F.: Escape dynamics in moderately damped Josephson junctions. *J. Low Temp. Phys.* **38**, 263 (2012)
180. Iansiti, M., Johnson, A., Smith, W.F., Rogalla, H., Lobb, C.J., Tinkham, M.: Charging energy and phase delocalization in single very small Josephson tunnel junctions. *Phys. Rev. Lett.* **59**, 489 (1987)
181. Iansiti, M., Tinkham, M., Johnson, A.T., Smith, W.F., Lobb, C.J.: Charging effects and quantum properties of small superconducting tunnel junctions. *Phys. Rev. B* **39**, 6465 (1989)
182. Inomata, K., Sato, S., Nakajima, K., Tanaka, A., Takano, Y., Wang, H.B., Nagao, M., Hatano, H., Kawabata, S.: Macroscopic quantum tunneling in a *d*-wave high- T_c BiSrCaCuO superconductor. *Phys. Rev. Lett.* **95**, 107005 (2005)
183. Jin, X.Y., Lisenfeld, J., Koval, Y., Lukashenko, A., Ustinov, A.V., Mueller, P.: Enhanced macroscopic quantum tunneling in BiSrCaCuO intrinsic Josephson-junction stacks. *Phys. Rev. Lett.* **96**, 177003 (2006)
184. Tzalenchuk, A.Ya., Lindstrom, T., Charlebois, S.A., Stepanov, E.A., Ivanov, Z., Zagoskin, A.M.: Mesoscopic Josephson junctions of high- T_c superconductors. *Phys. Rev. B* **68**, 100501 (2003)
185. Testa, G., Monaco, A., Esposito, E., Sarnelli, E., Kang, D.J., Mennema, S.H., Tarte, E.J., Blamire, M.G.: Midgap state-based π -junctions for digital applications. *Appl. Phys. Lett.* **85**, 1202 (2004)
186. Testa, G., Sarnelli, E., Monaco, A., Esposito, E., Eijnaes, M., Kang, D.J., Mennema, S.H., Tarte, E.J., Blamire, M.G.: Evidence of midgap-state-mediated transport in 45° symmetric[001]tilt- $\text{YBa}_2\text{Cu}_3\text{O}_{7-x}$ bicrystal grain-boundary junctions. *Phys. Rev. B* **71**, 134520 (2005)
187. Stornaiuolo, D., Gambale, E., Bauch, T., Born, D., Cedergren, K., Dalena, D., Barone, A., Tagliacozzo, A., Lombardi, F., Tafuri, F.: Underlying physical aspects of fluctuations in YBaCuO grain boundary Josephson junctions. *Physica C* **468**, 310 (2008)
188. Tagliacozzo, A., Born, D., Stornaiuolo, D., Gambale, E., Dalena, D., Lombardi, F., Barone, A., Altshuler, B.L., Tafuri, F.: Observation of mesoscopic conductance fluctuations in YBaCuO grain boundary Josephson junctions. *Phys. Rev. B* **75**, 012507 (2007)
189. Tagliacozzo, A., Tafuri, F., Gambale, E., Jouault, B., Born, D., Lucignano, P., Stornaiuolo, D., Lombardi, F., Barone, A., Altshuler, B.L.: Mesoscopic conductance fluctuations in YBCO grain boundary junction at low temperature. *Phys. Rev. B* **79**, 024501 (2009)
190. Lucignano, P., Stornaiuolo, D., Tafuri, F., Altshuler, B.L., Tagliacozzo, A.: Evidence of minigap in YBCO grain boundary Josephson junctions. *Phys. Rev. Lett.* **105**, 147001 (2010)
191. Lee, P.A., Ramakrishnan, T.V.: Disordered electronic systems. *Rev. Mod. Phys.* **57**, 287 (1985)
192. Lee, P.A., Stone, A.D.: Universal conductance fluctuations in metals. *Phys. Rev. Lett.* **55**, 1622 (1985)
193. Lee, P.A., Stone, A.D., Fukuyama, H.: Universal conductance fluctuations in metals: effects of finite temperature, interactions, and magnetic field. *Phys. Rev. B* **35**, 1039 (1987)
194. Altshuler, B.L., Lee, P.: Disordered electronic systems. *Phys. Today* **41**(12), 36 (1988)
195. Webb, R.A., Washburn, S.: Quantum interference fluctuations in disordered metals. *Phys. Today* **41**(12), 46 (1988)
196. Imry, Y.: *Introduction to Mesoscopic Physics*. Oxford University Press, Oxford (1997)
197. Gedik, N., Orenstein, J., Liang, R., Bonn, D.A., Hardy, W.N.: Diffusion of nonequilibrium quasi-particles in a cuprate superconductor. *Science* **300**, 1410 (2003)
198. Wang, J., Shi, C., Tian, M., Zhang, Q., Kumar, N., Jain, J.K., Mallouk, T.E., Chan, M.H.W.: Proximity-induced superconductivity in nanowires: minigap state and differential magnetoresistance oscillations. *Phys. Rev. Lett.* **102**, 247003 (2009)
199. Gross, R., Alff, L., Beck, A., Froehlich, O.M., Koelle, D., Marx, A.: Physics and technology of high temperature superconducting Josephson junctions. *IEEE Trans. Appl. Supercond.* **7**, 2929 (1997)
200. Gross, R., Mayer, B.: Transport processes and noise in YBaCuO grain boundary junctions. *Physica C* **180**, 235 (1991)
201. Moeckly, B.H., Lathrop, D.K., Buhman, R.A.: Electromigration study of oxygen disorder and grain-boundary effects in YBaCuO thin films. *Phys. Rev. B* **47**, 400 (1993)
202. Sarnelli, E., Testa, G., Esposito, E.: A two channel model as a possible microscopic configuration of the “barrier” in high T_c grain boundary junctions. *J. Supercond.* **7**, 387 (1994)
203. Kalisky, B., Kirtley, J.R., Nowadnick, E.A., Dinner, R.B., Zeldov, E., Ariando, Wenderich, S., Hilgenkamp, H., Feldmann, D.M., Moler, K.A.: Dynamics of single vortices in grain boundaries: I - V characteristics on the fermi-volt scale. *Appl. Phys. Lett.* **94**, 202504 (2009)
204. Gustafsson, D., Pettersson, H., Iandolo, B., Olsson, E., Bauch, T., Lombardi, F.: Soft nanostructuring of YBCO Josephson junctions by phase separation. *Nano Lett.* **10**, 4824 (2010)
205. Nagel, J., Kononenko, K.B., Kemmler, M., Turad, M., Werner, R., Kleisz, E., Menzel, S., Klingeler, R., Buchner, B., Kleiner, R., Koelle, D.: Resistively shunted YBCO grain boundary junctions and low-noise SQUIDs patterned by a focused ion

- beam down to 80 nm linewidth. *Supercond. Sci. Technol.* **24**, 015015 (2011)
206. Foley, C.P., Hilgenkamp, H.: Why nanoSQUIDs are important: an introduction to the focus issue. *Supercond. Sci. Technol.* **22**, 064001 (2009)
 207. Zaenen, J., Gunnarsson, O.: Charged magnetic domain lines and the magnetism of high- T_c oxides. *Phys. Rev. B* **40**, 7391 (1989)
 208. Tranquada, J.M., Buttrey, D.J., Sachan, V., Lorenzo, J.E.: Simultaneous ordering of holes and spins in $\text{La}_2\text{NiO}_{4.125}$. *Phys. Rev. Lett.* **73**, 1003 (1994)
 209. Kivelson, S.A., Bindloss, I.P., Fradkin, E., Oganessian, V., Tranquada, J.M., Kapitulnik, A., Howald, C.: How to detect fluctuating stripes in the high-temperature superconductors. *Rev. Mod. Phys.* **75**, 1201 (2003)
 210. Graser, S., Hirschfeld, P.J., Kopp, T., Gutser, R., Andersen, B.M., Mannhart, J.: How grain boundaries limit supercurrents in high-temperature superconductors. *Nat. Phys.* **6**, 609 (2010)
 211. Papari, G., Carillo, F., Stornaiuolo, D., Longobardi, L., Beltram, F., Tafuri, F.: High critical-current density and scaling of phase-slip processes in YBaCuO nanowires. *Supercond. Sci. Technol.* **25**, 035011 (2012)
 212. Papari, G., Carillo, F., Born, D., Bartoloni, L., Gambale, E., Stornaiuolo, D., Pingue, P., Beltram, F., Tafuri, F.: YBCO nanobridges: simplified fabrication process by using a Ti hard mask. *IEEE Trans. Appl. Supercond.* **19**, 183 (2009)
 213. Xu, K., Heath, J.R.: Long, highly-ordered high-temperature superconductor nanowire arrays. *Nano Lett.* **8**, 3845 (2008)
 214. Larsson, P., Nilsson, B., Ivanov, Z.G.: Fabrication and transport measurements of YBaCuO nanostructures. *J. Vac. Sci. Technol.* **18**, 25 (2000)
 215. Schneider, J., Kohlstedt, H., Wordenweber, R.: Nanobridges of optimized $\text{YBa}_2\text{Cu}_3\text{O}_7$ thin films for superconducting flux-flow type devices. *Appl. Phys. Lett.* **63**, 2426 (1993)
 216. Assink, H.P., v.d. Harg, A.J.M., Schep, C.M., Chen, N.Y., v.d. Marel, D., Hadley, P., v.d. Drift, E.W.J.M., Mooij, J.E.: Critical currents in submicron $\text{YBa}_2\text{Cu}_3\text{O}_7$ lines. *IEEE Trans. Appl. Supercond.* **3**, 2983 (1993)
 217. Mohanty, P., Wei, J.Y.T., Ananth, V., Morales, P., Skocpol, W.: Nanoscale high-temperature superconductivity. *Physica C* **666**, 408 (2004)
 218. Bonetti, J.A., Caplan, D.S., Van Harlingen, D.J., Weissman, B.: Electronic transport in underdoped $\text{YBa}_2\text{Cu}_3\text{O}_{7-\delta}$ nanowires: evidence for fluctuating domain structures. *Phys. Rev. Lett.* **93**, 87002 (2004)
 219. Herbstritt, F., Kemen, T., Marx, A., Gross, R.: Ultraviolet light assisted oxygenation process for submicron $\text{YBa}_2\text{Cu}_3\text{O}_{7-\delta}$ thin film devices. *J. Appl. Phys.* **91**, 5411 (2002)
 220. Carillo, F., Papari, G., Stornaiuolo, D., Born, D., Montemurro, D., Pingue, P., Beltram, F., Tafuri, F.: Little–Parks effect in single nanoscale YBaCuO rings. *Phys. Rev. B* **81**, 054505 (2010)
 221. Sochnikov, I., Shaulov, A., Yeshurun, Y., Logvenov, G., Bozovic, I.: Large oscillations of the magnetoresistance in nanopatterned high-temperature superconducting films. *Nat. Nanotechnol.* **5**, 516 (2010)
 222. Sochnikov, I., Bozovic, I., Shaulov, A., Yeshurun, Y.: Uncorrelated behavior of fluxoids in superconducting double networks. *Phys. Rev. B* **84**, 094530 (2011)
 223. Loder, F., Kampf, A.P., Kopp, T., Mannhart, J., Schneider, C.W., Barash, Y.S.: Magnetic flux periodicity of h/e in superconducting loops. *Nat. Phys.* **4**, 112 (2008)
 224. Loder, F., Kampf, A.P., Kopp, T.: Crossover from hc/e to $hc/2e$ current oscillations in rings of s-wave superconductors. *Phys. Rev. B* **78**, 174526 (2008)
 225. Barash, Y.S.: Low-energy subgap states and the magnetic flux periodicity in d -wave superconducting rings. *Phys. Rev. Lett.* **100**, 177003 (2008)
 226. Vakaryuk, V.: Universal mechanism for breaking the $hc/2e$ periodicity of flux-induced oscillations in small superconducting rings. *Phys. Rev. Lett.* **101**, 167002 (2008)
 227. Juricic, V., Herbut, I.F., Tesanovic, Z.: Restoration of the magnetic hc/e -periodicity in unconventional superconductors. *Phys. Rev. Lett.* **100**, 187006 (2008)
 228. Loder, F., Kampf, A.P., Kopp, T., Mannhart, J.: Flux periodicities in loops of nodal superconductors. *New J. Phys.* **11**, 075005 (2009)
 229. Berdiyrov, G.R., Milosevic, M.V., Latimer, M.L., Xiao, Z.L., Kwok, W.K., Peeters, F.M.: Large magnetoresistance oscillations in mesoscopic superconductors due to current-excited moving vortices. *Phys. Rev. Lett.* **109**, 057004 (2012)
 230. Fomin, V.M., Rezaev, R.O., Schmid, O.G.: Tunable generation of correlated vortices in open superconductor tubes. *Nano Lett.* **12**, 1282 (2012)
 231. Ribeiro Gomes, R., de Oliveira, I.G., Doria, M.M.: Little–Parks oscillations near a persistent current loop. *Phys. Rev. B* **85**, 144512 (2012)
 232. Liu, F.Y., Haviland, D.B., Glazman, L.I., Goldman, A.M.: Resistive transitions in ultrathin superconducting films: possible evidence for quantum tunneling of vortices. *Phys. Rev. Lett.* **68**, 2224 (1992)
 233. Yazdani, A., Kapitulnik, A., Beasley, M.R.: Observation of quantum dissipation in the vortex state of a highly disordered superconducting thin film. *Phys. Rev. Lett.* **76**, 1529 (1995)
 234. Tafuri, Kirtley, J.R., Born, D., Stornaiuolo, D., Medaglia, P.G., Orgiani, P., Balestrino, G., Kogan, V.G.: Dissipation in ultra-thin current-carrying superconducting bridges evidence for quantum tunneling of pearl vortices. *Europhys. Lett.* **73**, 948 (2006)
 235. Glazman, L.L., Fogel, N.Ya.: Possibility of quantum tunneling of vortices in thin superconducting films. *Sov. J. Low Temp. Phys.* **10**, 51 (1984) [*Fiz. Nizk. Temp.* **10**, 94 (1984)]
 236. Montemurro, D., Roddaro, S., Massarotti, D., Sorba, L., Beltram, F., Tafuri, F.: MIUR Prin-project “Nanowire high critical temperature superconductor field-effect devices (2011–2013)”. Unpublished (2012)
 237. Ahn, C.H., Bhattacharya, A., Di Ventra, M., Eckstein, J.N., Frisbie, C.D., Gershenson, M.E., Goldman, A.M., Inoue, I.H., Mannhart, J., Millis, A.J., Morpurgo, A.F., Natelson, D., Triscone, J.-M.: Electrostatic modification of novel materials. *Rev. Mod. Phys.* **78**, 1185 (2006)
 238. Salluzzo, M., Ghiringhelli, G., Cezar, J.C., Brookes, N.B., De Luca, G.M., Fracassi, F., Vaglio, R.: Indirect electric field doping of the CuO_2 planes of the cuprate $\text{NdBa}_2\text{Cu}_3\text{O}_7$ superconductor. *Phys. Rev. Lett.* **100**, 056810 (2008)
 239. Mannhart, J.: High- T_c transistors. *Supercond. Sci. Technol.* **9**, 49 (1996)
 240. Mourik, V., Zuo, K., Frolov, S., Plissard, S., Bakkers, E., Kouwenhoven, L.: Signatures of Majorana fermions in hybrid superconductor-semiconductor nanowire devices. *Science* **336**, 1003 (2012)
 241. Ovchinnikov, Y.N., Kresin, V.Z.: Theoretical investigation of Josephson tunneling between nanoclusters. *Phys. Rev. B* **61**, 2145050 (2010)
 242. Kresin, V.Z., Wolf, S.A.: Electron-lattice interaction and its impact on high- T_c superconductivity. *Rev. Mod. Phys.* **81**, 481 (2009)
 243. Lee, G.-H., Jeong, D., Choi, J.-H., Doh, Y.-J., Lee, H.-J.: Electrically tunable macroscopic quantum tunneling in a graphene-based Josephson junction. *Phys. Rev. Lett.* **107**, 146605 (2011)
 244. Jeong, D., Choi, J.-H., Lee, G.-H., Jo, S., Doh, Y.-J., Lee, H.-J.: Observation of supercurrent in PbIn–graphene–PbIn Josephson junction. *Phys. Rev. B* **83**, 094503 (2011)
 245. Ojeda-Aristizabal, C., Ferrier, M., Gueron, S., Bouchiat, H.: Tuning the proximity effect in a superconductor–graphene–superconductor junction. *Phys. Rev. B* **79**, 165436 (2009)

246. Borzenets, I.V., Coskun, U.C., Jones, S.J., Finkelstein, G.: Phase diffusion in graphene-based Josephson junctions. *Phys. Rev. Lett.* **107**, 137005 (2011)
247. Doh, Y.J., van Dam, J.A., Roest, A.L., Bakkers, E.P.A.M., Kouwenhoven, L.P., De Franceschi, S.: Tunable supercurrent through semiconductor nanowires. *Science* **309**, 272 (2005)
248. Xiang, J., Vidan, A., Tinkham, M., Westervelt, R.M., Lieber, C.M.: Ge/Si nanowire mesoscopic Josephson junctions. *Nat. Nanotechnol.* **1**, 208 (2006)
249. Jarillo-Herrero, P., van Dam, J.A., Kouwenhoven, L.P.: Quantum supercurrent transistors in carbon nanotubes. *Nature* **439**, 953 (2006)
250. Cleuziou, W., Wernsdorfer, J.P., Bouchiat, V., Ondarcuhu, T., Monthieux, M.: Carbon nanotube superconducting quantum interference device. *Nat. Nanotechnol.* **1**, 53 (2006)
251. Katsaros, G., Spathis, P., Stoffel, M., Fournel, F., Mongillo, M., Bouchiat, V., Lefloch, F., Rastelli, A., Schmidt, O.G., De Franceschi, S.: Hybrid superconductor, a semiconductor devices made from self-assembled SiGe nanocrystals on silicon. *Nat. Nanotechnol.* **5**, 458 (2010)
252. Courtois, H., Meschke, M., Peltonen, J.T., Pekola, J.P.: Origin of hysteresis in a proximity Josephson junction. *Phys. Rev. Lett.* **101**, 067002 (2008)
253. Angers, L., Chiodi, F., Montambaux, G., Ferrier, M., Guron, S., Bouchiat, H., Cuevas, J.C.: Proximity dc squids in the long-junction limit. *Phys. Rev. B* **77**, 165408 (2008)
254. Sahu, M., Bae, M.H., Rogachev, A., Pekker, D., Wei, T.C., Shah, N., Goldbart, P.M., Bezryadin, A.: Individual topological tunnelling events of a quantum field probed through their macroscopic consequences. *Nat. Phys.* **5**, 503 (2009)
255. Li, P., Wu, P.M., Bomze, Y., Borzenets, I.V., Finkelstein, G., Chang, A.M.: Switching currents limited by single phase slips in one-dimensional superconducting Al nanowires. *Phys. Rev. Lett.* **107**, 137004 (2011)
256. Li, P., Wu, P.M., Bomze, Y., Borzenets, I.V., Finkelstein, G., Chang, A.M.: Retrapping current, self-heating, and hysteretic current–voltage characteristics in ultranarrow superconducting aluminum nanowires. *Phys. Rev. B* **84**, 184508 (2011)
257. Tinkham, M., Free, J.U., Lau, C.N., Markovic, N.: Hysteretic I-V curves of superconducting nanowires. *Phys. Rev. B* **68**, 134515 (2003)
258. Shah, N., Pekker, D., Goldbart, P.M.: Inherent stochasticity of superconductor–resistor switching behavior in nanowires. *Phys. Rev. Lett.* **101**, 207001 (2008)
259. Little, W.A.: Decay of persistent currents in small superconductors. *Phys. Rev.* **156**, 396 (1967)
260. Langer, J.S., Ambegaokar, V.: Intrinsic resistive transition in narrow superconducting channels. *Phys. Rev.* **164**, 498 (1967)
261. McCumber, D.E., Halperin, B.I.: Time scale of intrinsic resistive fluctuations in thin superconducting wires. *Phys. Rev. B* **1**, 1054 (1970)
262. Giordano, N.: Evidence for macroscopic quantum tunneling in one-dimensional superconductors. *Phys. Rev. Lett.* **61**, 2137 (1988)
263. Bezryadin, A., Lau, C.N., Tinkham, M.: Quantum suppression of superconductivity in ultrathin nanowires. *Nature* **404**, 971 (2000)
264. Lau, C.N., Markovic, N., Bockrath, M., Bezryadin, A., Tinkham, M.: Quantum phase slips in superconducting nanowires. *Phys. Rev. Lett.* **87**, 217003 (2001)
265. Rogachev, A., Bollinger, A.T., Bezryadin, A.: Influence of high magnetic fields on the superconducting transition of one-dimensional Nb and MoGe nanowires. *Phys. Rev. Lett.* **94**, 017004 (2005)
266. Altomare, F., Chang, A.M., Melloch, M.R., Hong, Y., Tu, C.W.: Evidence for macroscopic quantum tunneling of phase slips in long one-dimensional superconducting Al wires. *Phys. Rev. Lett.* **97**, 017001 (2006)